ORNL/SPR-2021/2093

Fuel Assembly Reference Information for SNF Radiation Source Term Calculations

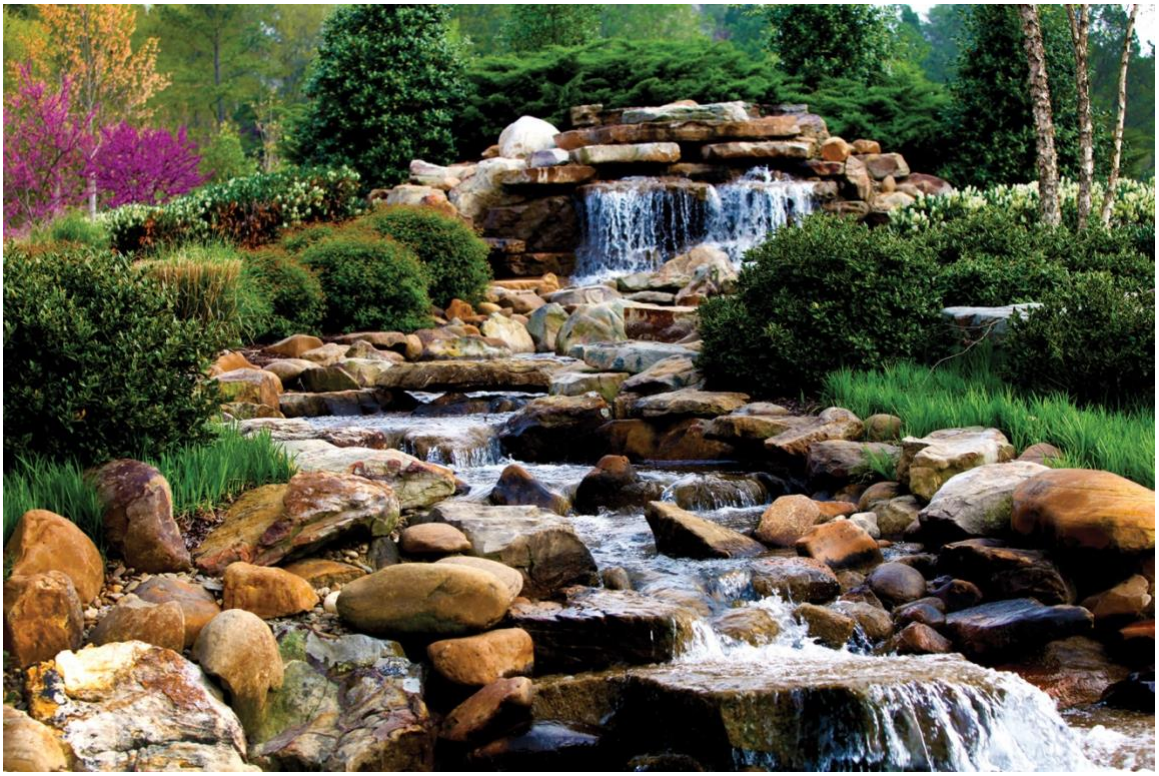

Georgeta Radulescu
Brandon R. Grogan
Kaushik Banerjee

September 2021

OAK RIDGE National Laboratory

ORNL IS MANAGED BY UT-BATTELLE LLC FOR THE US DEPARTMENT OF ENERGY

DOCUMENT AVAILABILITY

Reports produced after January 1, 1996, are generally available free via US Department of Energy (DOE) SciTech Connect.

Website www.osti.gov

Reports produced before January 1, 1996, may be purchased by members of the public from the following source:

National Technical Information Service
5285 Port Royal Road
Springfield, VA 22161
Telephone 703-605-6000 (1-800-553-6847)
TDD 703-487-4639
Fax 703-605-6900
E-mail info@ntis.gov
Website http://classic.ntis.gov/

Reports are available to DOE employees, DOE contractors, Energy Technology Data Exchange representatives, and International Nuclear Information System representatives from the following source:

Office of Scientific and Technical Information
PO Box 62
Oak Ridge, TN 37831
Telephone 865-576-8401
Fax 865-576-5728
E-mail reports@osti.gov
Website http://www.osti.gov

This report was prepared as an account of work sponsored by an agency of the United States Government. Neither the United States Government nor any agency thereof, nor any of their employees, makes any warranty, express or implied, or assumes any legal liability or responsibility for the accuracy, completeness, or usefulness of any information, apparatus, product, or process disclosed, or represents that its use would not infringe privately owned rights. Reference herein to any specific commercial product, process, or service by trade name, trademark, manufacturer, or otherwise, does not necessarily constitute or imply its endorsement, recommendation, or favoring by the United States Government or any agency thereof. The views and opinions of authors expressed herein do not necessarily state or reflect those of the United States Government or any agency thereof.

ORNL/SPR-2021/2093

Nuclear Energy and Fuel Cycle Division

FUEL ASSEMBLY REFERENCE INFORMATION FOR SNF RADIATION SOURCE TERM CALCULATIONS

Georgeta Radulescu
Brandon R. Grogan
Kaushik Banerjee

Date Published: September 2021

Prepared by
OAK RIDGE NATIONAL LABORATORY
Oak Ridge, TN 37831-6283
managed by
UT-BATTELLE, LLC
for the
US DEPARTMENT OF ENERGY
under contract DE-AC05-00OR22725

CONTENTS

LIST OF TABLES

ABBREVIATIONS

APSRA	axial power-shaping rod assembly
ATCR	accident-tolerant control rod
ATF	accident-tolerant fuel
B&W	Babcock & Wilcox
BAA	burnable absorber assembly
BPR	burnable poison rod
BPRA	burnable poison rod assembly
BWR	boiling water reactor
CE	Combustion Engineering
CEA	control element assembly
CRA	control rod assembly
CRC	commercial reactor criticality
EBC	equivalent boron content
EFPD	effective full-power day
GC	General Counsel
GE	General Electric
GP	gas plenum
ID	inner diameter
IFBA	integral fuel burnable absorber
LEF	lower end fitting
LWR	light water reactor
NEI	Nuclear Energy Institute
NFH	non-fuel hardware
NSA	neutron source assemblies
OD	outer diameter
PCI	pellet-clad interaction
ppmB	parts per million boron
PWR	pressurized water reactor
RCCA	rod cluster control assembly
SNF	spent nuclear fuel
TPD	thimble plug device
UEF	upper end fitting
WABA	wet annular burnable absorber
WE	Westinghouse
YMP	Yucca Mountain Project

ABSTRACT

This report consolidates publicly available information related to pressurized water reactor (PWR) and boiling water reactor (BWR) nuclear fuel physical characteristics and operating conditions. The intent of this report is to provide reference information for use in shielding analyses of spent nuclear fuel transportation packages and storage casks. Most data are dated 1992 or older. Specific information provided in this report includes:

- physical characteristics of main assembly classes Babcock & Wilcox 15 × 15; Combustion Engineering 14 × 14 and 16 × 16; Westinghouse 14 × 14, 15 × 15, and 17 × 17; BWR/4-6 7 × 7, 8 × 8, 9 × 9, and 10 × 10; and physical characteristics of site-specific fuel assemblies for the Haddam Neck, Indian Point Unit 1, Palisades, San Onofre Unit 1, Yankee Rowe, Big Rock Point, and Dresden Unit 1 power reactors;
- representative PWR and BWR nuclear fuel operating conditions;
- axial burnup profiles that are bounding in regard to radial dose rates of PWR and BWR fuel assemblies;
- physical characteristics and operating conditions of non-fuel hardware (NFH); and
- data related to the Co activation source in fuel and NFH materials, including Co impurity concentrations in various steel and Inconel alloys and ORIGEN flux scaling factors.

1. INTRODUCTION

This report provides reference information for pressurized water reactor (PWR) and boiling water reactor (BWR) fuel assemblies for use in spent nuclear fuel (SNF) radiation source term and dose rate calculations. The information consolidated in this report includes publicly available light water reactor (LWR) fuel assembly design data dated 1992 or older. Available information is provided for main fuel assembly designs and non-fuel hardware (NFH), as well as for representative nuclear fuel operating conditions. Principal publicly available documents that provide the information summarized in this report include:

- *Characteristics of Potential Repository Waste*, DOE/RW-0184-R1 [1];
- *Characteristics of Spent Fuel, High Level Waste, and Other Radioactive Wastes which May Require Long-Term Isolation*, DOE/RW-0184, Appendix 2A, Physical Descriptions of LWR Fuel Assemblies [2];
- *Characteristics of Spent Fuel, High-Level Waste, and other Radioactive Wastes which May Require Long-Term Isolation*, DOE/RW-0184, Appendix 2E, "Physical Descriptions of LWR Nonfuel Assembly Hardware" [3];
- *Physical Characteristics of Non-Fuel Assembly Reactor Components*, PNL-8425 [4];
- *Physical Characteristics of the GE BWR Fuel Assemblies*, ORNL/TM-10902 [5];
- *Physical and Decay Characteristics of Commercial LWR Spent Fuel*, ORNL/TM-9591 [6];
- Commercial reactor criticality (CRC) data reports prepared for the Yucca Mountain Project (YMP) [7, 8, 9, 10];
- *Axial Burnup Profile Database for Pressurized Water Reactors*, YAEC-1937 [11];
- *BWR Axial Burnup Profile Evaluation*, Framatome ANP 32-5045751-00 [12];
- *Spent Fuel Assembly Hardware: Characterization and 10CFR 61 Classification for Waste Disposal*, PNL-6906-vol. 1 [13]; and
- *Nuclear Fuel Data Survey Form GC-859*, Energy Information Administration, US Department of Energy, http://www.eia.gov/survey/form/gc_859/proposed/form.pdf (accessed September 30, 2020) [14].

Section 2 provides data on the physical characteristics of main assembly classes Babcock & Wilcox (B&W) 15 × 15; Combustion Engineering (CE) 14 × 14 and 16 × 16; Westinghouse (WE) 14 × 14, 15 × 15, and 17 × 17; BWR/4-6 assembly classes 7 × 7, 8 × 8, 9 × 9, and 10 × 10; and data on site-specific fuel assemblies for the Haddam Neck, Indian Point Unit 1, Palisades, San Onofre Unit 1, Yankee Rowe, Big Rock Point, and Dresden Unit 1 power reactors. Data are provided for the active fuel and fuel hardware regions of the PWR and BWR fuel assembly classes. The fuel hardware regions include the assembly upper end fitting (UEF), gas plenum (GP), and lower end fitting (LEF). Sections 3 and 4 provide representative nuclear fuel operating conditions and bounding axial burnup profiles for PWR and BWR fuel, respectively. Section 5 provides physical characteristics and operating conditions of NFH, such as control rods and burnable poison rods. NFH is not an integral part of the fuel assembly, but irradiated PWR NFH components are usually inserted into the guide tubes of the PWR SNF assemblies loaded in storage canisters. Section 6 provides data related to the Co activation source in fuel hardware and NFH materials, including Co impurity concentrations in various steel and Inconel alloys and ORIGEN flux scaling factors. Section 7 provides conclusions and recommendations.

2. PHYSICAL CHARACTERISTICS OF FUEL ASSEMBLIES

As of 2013, over 245,000 SNF assemblies have been discharged in the United States [15], based on the industry-provided General Counsel (GC)-859 survey data [14]. Many changes have occurred in assembly design since the beginning of commercial power in 1957. These changes were instituted to address shortcomings in older designs, improve the performance of the fuel, decrease downtime, and increase burnup. One of the more obvious changes in the assembly designs is an increase in the array sizes. PWR designs are fixed at reactor construction by the shape of the control rod assemblies. Nevertheless, the typical PWR designs have shifted from 14 × 14 and 15 × 15 arrays in early reactors to 17 × 17 arrays in more modern designs. In BWRs, the cruciform control blades allow for changes in the overall assembly geometry. BWR assemblies have moved from 6 × 6 and 7 × 7 assemblies to 10 × 10 designs. BWR assemblies have added water rods and channels in the center to provide a source of non-boiling water for additional cooling and increased neutron moderation [16]. From early fuel with no water rods, these water channels have grown larger with each passing generation, increasing from a single fuel rod location in the GE-3 assembly type [5] to large channels that displace eight to nine fuel rods in designs such as the GE-14 or Atrium-10 designs [17].

The desire for increased burnup has necessitated an increase in the average enrichment of the fuel from around 2% in early reactors to nearly 5% today [5]. This increase in initial enrichments also increases the initial excess reactivity of the assemblies. Design changes in the fuel loading patterns were made to decrease the initial reactivity and peaking power across the reactor core. In PWRs, this is accomplished largely by using Gd-doped fuel rods interspersed in the assemblies. In some assembly designs, the fuel pellets are also given a coating of ZrB_2, which burns off during the first cycle in the reactor [18]. To accommodate more fission gases in high-burnup fuel, the length of the PWR fuel rod was slightly increased, and the thicknesses of the assembly top and bottom nozzles were reduced [19]. For extended-burnup fuel, UO_2 with a grain size larger than that of the standard fuel was produced by adding certain dopants (e.g., Cr_2O_3) [20]. The fission gas release rate decreases and internal pressure within a fuel pin increases more slowly in UO_2 fuel with larger grain size.

For BWRs, fuel loading patterns are even more complicated. Most modern BWR assemblies contain several partial length rods that decrease the two-phase pressure drop for improved thermal/hydraulic performance and mitigate the loss of shutdown margin [16]. Most full-length BWR fuel rods and some PWR fuel rods include a natural uranium or low enrichment region at the top and bottom of the fuel stack called blanket. These blankets lead to reduced axial leakage and improved U utilization in the assembly [21]. Blanketed fuel assemblies also have a higher axial power peaking than non-blanketed fuel with the same average assembly burnup [21]. In most BWR assemblies, rods near water holes and the periphery of the assembly start with a lower enrichment due to the increased neutron moderation in these regions [16]. Finally, modern BWR designs use axial zoning of the enrichment and integral burnable absorber (e.g., Gd_2O_3) loadings to hold down the initial power level and minimize peaking in the center of the assembly [16].

For the cladding, one of the first and almost immediate changes in the fuel design was a shift from stainless-steel cladding to a Zr alloy, Zircaloy. The Zircaloy cladding was much more corrosion resistant and produced fewer activation products. In modern PWRs with high burnups, standard Zircaloy cladding is problematic because of corrosion. New high-performance fuel cladding materials—such as the ZIRLO alloy developed by WE and the M5 alloy developed by Framatome—are used in newer PWR assemblies [22]. Zircaloy corrosion has not been a significant issue with BWRs; however, pellet-clad interaction (PCI) led to the development of barrier cladding during the 1980s, which significantly reduced the frequency of reported PCI failures [23]. Fuel hardware has also evolved alongside fuel designs. For example, changes to the shape of spacer grids provide better mechanical properties, such as fewer

cladding failures due to vibrations, and also improve cooling by providing better water mixing as it passes through each spacer.

This section presents publicly available data for PWR and BWR fuel assemblies. Most PWR assembly design information were obtained from Appendix 2A, "Physical Descriptions of LWR Fuel Assemblies," of the DOE/RW-0184 report [2]. Most BWR assembly design data were obtained from the ORNL/TM-10902 report [5]. Assembly design information from the ORNL/TM-9591 and CRC data reports [6–10] were also used. The ranges of initial U weight, enrichment, and assembly average burnup presented in this report are based on the GC-859 survey data [14] incorporated in the Used Nuclear Fuel Storage, Transportation, and Disposal Analysis Resource and Data System [24]. The GC-859 fuel assembly type codes [14] are used in the tables.

Physical characteristics are provided for:

- PWR assembly classes B&W 15 × 15, CE 14 × 14, and 16 × 16 and WE 14 × 14, 15 × 15, and 17 × 17;
- BWR/4-6 assembly classes 7 × 7, 8 × 8, 9 × 9, and 10 × 10; and
- site-specific fuel assemblies for the Haddam Neck, Indian Point Unit 1, Palisades, San Onofre Unit 1, Yankee Rowe, Big Rock Point, and Dresden Unit 1 power reactors.

The assembly classes and the overall length and width of the fuel assemblies in these classes [1] are presented in Table 1. Sections 2.1 and 2.2 present data for the active fuel and fuel hardware regions of PWR and BWR fuel assembly designs, respectively. These data are provided for representative fuel assembly designs within the assembly classes and for the site-specific fuel assemblies. The GC-859 fuel assembly type codes [14] are used to identify the fuel assembly designs described in Sections 2.1 and 2.2. Useful fuel design information is also available in NUREG-1754 [25].

Table 1. Main assembly classes and assembly overall dimensions.

Assembly class	Reactor type	Assembly length (cm)	Assembly width (cm)
Non-site-specific assembly classes			
B&W 15 × 15	PWR	420.875	21.6916
BWR/4–6	BWR	447.548	13.8176
CE 14 × 14	PWR	398.78	20.574
CE 16 × 16	PWR	449.072	20.574
WE 14 × 14	PWR	405.892	19.7104
WE 15 × 15	PWR	405.892	21.4378
WE 17 × 17	PWR	405.892	21.4378
Site-specific assembly classes			
Haddam Neck	PWR	348.234	21.3868
Indian Point Unit 1	PWR	352.552	15.9258
Palisades	PWR	374.65	20.828
San Onofre Unit 1	PWR	348.234	19.7104
Yankee Rowe	PWR	283.972	19.3548
Big Rock Point	BWR	213.36	16.5608
Dresden Unit 1	BWR	341.376	10.8712
LaCrosse	BWR	260.35	14.2748

A typical fuel assembly model for dose rate calculations has several axial regions. At a minimum, the axial zones include a LEF region, an active fuel region, a GP region, and an UEF region. The fuel assembly hardware regions are typically represented as cuboids with homogeneous material and a ^{60}Co activation source. The material mixture composition and mass density in each fuel hardware region are derived from the material weights and the bounding volume of the region. The ^{60}Co activation source strength depends on the assumed initial concentration of the ^{59}Co impurity in hardware materials, hardware material weights, neutron flux level and energy spectrum at the fuel hardware location, and the irradiation duration. The non-fuel materials and their weights for each fuel assembly axial region were obtained from Appendix 2A of the DOE/RW-0184 report [2], which is the only publicly available document that provides this type of information. Unless otherwise indicated, the lengths of the assembly LEF, GP, and UEF for most fuel assembly types were inferred from the assembly drawings provided in the same report [2]. Those drawings do not specifically provide the lengths of the assembly LEF, GP, and UEF. The length of the assembly LEF is defined as the length of the fuel assembly below the active fuel. The length of the assembly GP is defined as the length of the fuel assembly between the tip of the fuel rods and the top of the active fuel. The length of the assembly UEF was defined as the remainder of the fuel assembly length. Therefore, the lengths provided in this report for the assembly LEF, GP, and UEF regions could be approximate.

2.1 PWR FUEL ASSEMBLIES

Section 2.1.1 presents data for the active fuel region, and Section 2.1.2 provides data for the hardware regions of the main PWR fuel assembly classes.

2.1.1 PWR Fuel Region Characteristics

This section presents the characteristics of the active fuel region of the assembly classes B&W 15 × 15 (Table 2); CE 14 × 14 and 16 × 16 (Table 3); and WE 14 × 14, 15 × 15, and 17 × 17 (Table 4), as well as site-specific assembly classes Haddam Neck (Table 5), Indian Point-1, Palisades, San Onofre-1, and Yankee Rowe (Table 6).

Table 2. Fuel region characteristics for the B&W 15 × 15 assembly class.

GC-859 assembly type code (Fuel design)	B1515B3 (Mark B3)	B1515B4 (Mark B4)	B1515B4Z (Mark B4Z)	B1515B8 (Mark B8)	B1515B9 (Mark B9)	B1515B10 (Mark B10)
Array size	15 × 15	15 × 15	15 × 15	15 × 15	15 × 15	15 × 15
Initial ^{235}U enrichment mean (wt %)	2.45	3.24	3.84	3.65	3.96	3.90
Initial ^{235}U enrichment range (wt %)	1.93–2.84	1.98–4.73	3.22–3.95	3.29–4.01	3.29–4.76	3.24–4.73
Average initial U mass (kg)	463.91	464.47	463.61	464.85	461.90	476.75
Initial U weight range (kg)	459.58–465.83	462.47–491.72	455.71–466.31	457.01–468.56	462.97–467.57	461.04–489.30
Active fuel rod length (cm)	360.172	360.172	360.172	360.172	357.111	357.111
Number of fuel rods	208	208	208	208	208	208
Rod pitch (cm)	1.44272	1.44272	1.44272	1.44272	1.44272	1.44272
Clad material	Zircaloy-4	Zircaloy-4	Zircaloy-4	Zircaloy-4	Zircaloy-4	Zircaloy-4
Clad OD [a] (cm)	1.0922	1.0922	1.0922	1.0922	1.0922	1.0922
Clad thickness (cm)	0.06731	0.06731	0.06731	0.06731	0.06731	0.06731
Fuel pellet diameter (cm)	0.936244	0.936244	0.936244	0.936244	0.9398	0.9398
Number of guide/ instrument tubes	17	17	17	17	17	17
Guide tube material	Zircaloy-4	Zircaloy-4	Zircaloy-4	Zircaloy-4	Zircaloy-4	Zircaloy-4
Guide tube OD (cm)	1.3462	1.3462	1.3462	1.3462	1.3462	1.3462
Guide tube ID [b] (cm)	1.26492	1.26492	1.26492	1.26492	1.26492	1.26492
Instrument tube material	Zircaloy-4	Zircaloy-4	Zircaloy-4	Zircaloy-4	Zircaloy-4	Zircaloy-4
Instrument tube OD (cm)	1.3462	1.3462	1.3462	1.3462	1.3462	1.3462
Instrument tube ID (cm)	1.26492	1.26492	1.26492	1.26492	1.26492	1.26492

[a] *OD* stands for *outer diameter*.
[b] *ID* stands for *inner diameter*.

Table 3. Fuel region characteristics for assembly classes CE 14 × 14 and CE 16 × 16.

GC-859 assembly type code (Fuel design)	C1414A (CE 14 × 14 ANF)	C1414C (CE 14 × 14 CE)	C1414W (CE 14 × 14 WE)	C1616CSD (CE 16 × 16 CE)
Array size	14 × 14	14 × 14	14 × 14	16 × 16
Initial ^{235}U enrichment mean (wt %)	3.72	3.23	3.85	3.64
Initial ^{235}U enrichment range (wt %)	0.30–4.49	1.92–4.49	2.01–4.67	1.87–4.63
Average initial U mass (kg)	387.83	381.97	403.50	413.82
Initial U range (kg)	343.42–412.28	323.22–408.51	382.77–411.72	394.41–433.20
Active fuel rod length (cm)	347.22	347.22	347.22	381
Number of fuel rods	176	176	176	236
Rod pitch (cm)	1.4732	1.4732	1.4732	1.286
Clad material	Zircaloy-4	Zircaloy-4	Zircaloy-4	Zircaloy-4
Clad OD (cm)	1.1176	1.1176	1.1176	0.9703
Clad thickness (cm)	0.07874	0.07112	0.06604	0.06351
Fuel pellet diameter (cm)	0.9398	0.95631	0.96647	0.8255
Number of guide/ instrument tubes	5	5	5	5
Guide tube material	Zircaloy-4	Zircaloy-4	Zircaloy-4	Zircaloy-4
Guide tube OD (cm)	2.8321	2.8321	2.8321	2.4892
Guide tube ID (cm)	2.6289	2.6289	2.6289	2.286
Instrument tube material	Zircaloy-4	Zircaloy-4	Zircaloy-4	Zircaloy-4
Instrument tube OD (cm)	2.8321	2.8321	2.8321	2.4892
Instrument tube ID (cm)	2.6289	2.6289	2.6289	2.286

Table 4. Fuel region characteristics for assembly classes WE 14 × 14, WE 15 × 15, and WE 17 × 17.

GC-859 assembly type code (Fuel design)	W1414WL (14 × 14 WE LOPAR)	W1515WL (15 × 15 WE LOPAR)	W1717WL (17 × 17 WE LOPAR) [a]	W1717WO (17 × 17 WE OFA) [a]
Array size	14 × 14	15 × 15	17 × 17	17 × 17
Initial ^{235}U enrichment mean (wt %)	3.64	3.47	3.68	4.59
Initial ^{235}U enrichment range (wt %)	2.27–4.97	1.40–4.95	1.60–4.95	3.61–4.81
Average initial U mass (kg)	397.41	455.06	459.52	421.49
Initial U weight range (kg)	382.13–405.81	437.50–465.60	419.1–469.2	387.40–429.58
Active fuel rod length (cm)	365.76	365.76	365.76	365.76
Number of fuel rods	179	204	264	264
Rod pitch (cm)	1.41224	1.43002	1.25984	1.25984
Clad material	Zircaloy-4	Zircaloy-4	Zircaloy-4	Zircaloy-4
Clad OD (cm)	1.07188	1.07188	0.94996	0.9144
Clad thickness (cm)	0.06172	0.06172	0.05715	0.05715
Fuel pellet diameter (cm)	0.92939	0.929386	0.81915	0.784352
Number of guide/ instrument tubes	17	21	25	25
Guide tube material	Zircaloy-4	Zircaloy-4	Zircaloy-4	Zircaloy-4
Guide tube OD (cm)	1.36906	1.38684	1.22428/1.08966	1.20396/1.08966
Guide tube ID (cm)	1.2827	1.30048	1.143/1.00838	1.12268/1.00838
Instrument tube material	Zircaloy-4	Zircaloy-4	Zircaloy-4	Zircaloy-4
Instrument tube OD (cm)	1.36906	1.38684	1.22428	1.20396
Instrument tube ID (cm)	1.2827	1.30048	1.143	1.12268

[a] These assemblies have a smaller guide tube diameter in the lower portion of the assembly.

Table 5. Fuel region characteristics for the Haddam Neck 15 × 15 assembly class.

GC-859 assembly type code (Fuel design)	XHN15B (B&W SS)	XHN15BZ (B&W Zr)	XHN15W (WE SS)	XHN15WZ (WE Zr)
Array size	15 × 15	15 × 15	15 × 15	15 × 15
Initial ^{235}U enrichment mean (wt %)	3.99	3.80	3.59	4.39
Initial ^{235}U enrichment range (wt %)	3.00–4.02	3.40–3.91	3.02–4.00	4.20–4.60
Average initial U mass (kg)	411.89	363.92	415.56	384.89
Initial uranium weight range (kg)	335.91–415.06	356.89–368.07	409.17–421.23	383.80–386.69
Active fuel rod length (cm)	306.07	306.07	309.372	306.07
Number of fuel rods	204	204	204	204
Rod pitch (cm)	1.43002	1.43002	1.43002	1.43002
Clad material	SS304 [a]	Zircaloy-4	SS304	Zircaloy-4
Clad OD (cm)	1.07188	1.07188	1.07188	1.07188
Clad thickness (cm)	0.04191	0.04191	0.04191	0.04191
Fuel pellet diameter (cm)	0.97155	0.97155	0.98933	0.97155
Number of guide/ instrument tubes	21	21	21	21
Guide tube material	SS304	SS304	SS304	SS304
Guide tube OD (cm)	1.3462	1.3462	1.3462	1.3462
Guide tube ID (cm)	1.26492	1.26492	1.26492	1.26492
Instrument tube material	SS304	SS304	SS304	SS304
Instrument tube OD (cm)	1.3462	1.3462	1.3462	1.3462
Instrument tube ID (cm)	1.26492	1.26492	1.26492	1.26492

[a] Stainless steel type 304.

Table 6. Fuel region characteristics for site-specific assembly classes Indian Point-1 (XIP14W), Palisades (XPA15C), San Onofre-1 (XSO14W), and Yankee Rowe (XYR16C).

GC-859 assembly type code (Fuel design)	XIP14W (Indian Point-1 13 × 14 WE)	XPA15C (Palisades 15 × 15 CE)	XSO14W (San Onofre-1 14 × 14 WE)	XYR16C (Yankee Rowe 15 × 16 CE)
Array size	13 × 14	15 × 15	14 × 14	15 × 16
Initial ^{235}U enrichment mean (wt %)	4.12	2.47	3.87	3.80
Initial ^{235}U enrichment range (wt %)	2.83–4.36	1.65–3.06	3.16–4.02	3.51–3.92
Average initial U mass (kg)	191.15	412.44	368.15	228.77
Initial U range (kg)	174.78–200.47	404.55–416.78	359.75–374.89	217.60–233.40
Active fuel rod length (cm)	254.6604	335.28	304.8	231.14
Number of fuel rods	180	204	180	231
Rod pitch (cm)	1.12014	1.397	1.41224	1.1989
Clad material	SS304 [a]	Zircaloy-4	SS304	Zircaloy-4
Clad OD (cm)	0.86741	1.06172	1.07188	0.93243
Clad thickness (cm)	0.07239	0.06604	0.04191	0.0635
Fuel pellet diameter (cm)	0.97409	0.90932	0.97409	0.78867
Number of guide/ instrument tubes	16	1	16	9
Guide tube material	SS304	Zircaloy-4	SS304	Zircaloy-4
Guide tube OD (cm)	0.86741	1.397	1.36906	0.93243
Guide tube ID (cm)	0	0	1.2827	0
Instrument tube material	SS304	Zircaloy-4	SS304	Zircaloy-4
Instrument tube OD (cm)	0.86741	1.397	1.36906	0.93243
Instrument tube ID (cm)	0	0	1.2827	0

[a] Stainless steel type 304.

Fuel region characteristics of Haddam Neck fuel assemblies are provided in Table 5. The array size of the Haddam Neck fuel assembly is 15 × 15, and the total length is 348.234 cm (137.1 in). However, there are various versions of the Haddam Neck fuel assembly manufactured by different nuclear fuel vendors. The information is provided for four assembly versions with stainless steel and Zircaloy-4 cladding manufactured by B&W and WE fuel vendors.

2.1.2 PWR Fuel Assembly Hardware Data

This section presents the characteristics of NFH regions of the assembly class B&W 15 × 15 (Table 7); assembly types C1414A (Table 8), C1414C (Table 9), C1414W (Table 10), C1616CSD (Table 11), W1414WL (Table 12), W1515WL (Table 13), W1717WL (Table 14), and W1717WO (Table 15); and site-specific assembly classes Haddam Neck (Table 16 and Table 17), Palisades (Table 18), San Onofre-1 (Table 18), and Yankee Rowe (Table 19).

Table 7. Fuel assembly hardware dimensions and materials for the B&W 15 × 15 assembly class.

Axial fuel assembly zone	Length [a] (cm)	Assembly parts in the zone	Material	Weight (kg/assembly)
UEF	24.819 [b]/ 25.794 [c]	Top nozzle	SS CF3M	7.48
		Spring retainer	SS CF3M	0.91
		Hold-down spring	Inconel-718	1.8
		Upper end plug	SS 304	0.06
		Upper nut	SS 304L	0.51
GP	19.161 [b]/ 21.247 [c]	Spacer (plenum)	Inconel-718	1.04
Active Fuel	360.172 [b]/ 357.111 [c]	Guide tubes	Zircaloy-4	8
		Instrument tube	Zircaloy-4	0.64
		Spacer (in core)	Inconel-718 [d]/ Zircaloy-4 [e]	4.9
		Grid supports	Zircaloy-4	0.64
LEF	16.723	Bottom nozzle	SS CF3M	8.16
		Spacer (bottom)	Inconel-718	1.3
		Lower nut	SS 304	0.15

[a] Lengths of the LEF, active fuel, and GP from [8].
[b] Assembly codes B1515B3, B1515B4, B1515B4Z, and B1515B8.
[c] Assembly codes B1515B9 and B1515B10.
[d] Assembly codes B1515B3 and B1515B4.
[e] Assembly codes B1515B4Z, B1515B8, B1515B9 and B1515B10.

Table 8. Fuel assembly hardware dimensions and materials for the C1414A assembly.

Axial fuel assembly zone	Length (cm)	Assembly parts in the zone	Material	Weight (kg/assembly)
UEF	19.3024	Top nozzle	SS-ANF	7.31
		Hold-down spring	Inconel X-750	1.41
		Guide tube hardware	Zircaloy-4	0.29016
			Inconel X-750	2.82984
GP	26.068	Spacer (plenum)	Zircaloy-4	0.5518
			Inconel-718	0.0682
Active Fuel	347.22	Guide tubes	Zircaloy-4	9.82
		Spacer (in core)	Inconel-718	0.5681
			Zircaloy-4	4.3719
LEF	6.7996	Bottom nozzle	SS-ANF	6.08

Table 9. Fuel assembly hardware dimensions and materials for the C1414C assembly.

Axial fuel assembly zone	Length (cm)	Assembly parts in the zone	Material	Weight (kg/assembly)
UEF	16.84	Locking posts	SS 304	2.63
		Hold-down spring	CE Ni Alloy	1.1
		Flow plate	SS 304	1.45
		Hold-down plate	SS 304	1
GP	26.07	Spacer (plenum)	Zircaloy-4	0.68
Active Fuel	347.22	Guide tubes	Zircaloy-4	11.8
		Spacer (lower)	Inconel 625	1.36
		Spacer (in core)	Zircaloy-4	4.76
LEF	7.94	Bottom nozzle	SS 304	5

Table 10. Fuel assembly hardware dimensions and materials for the C1414W assembly.

Axial fuel assembly zone	Length (cm)	Assembly parts in the zone	Material	Weight (kg/assembly)
UEF	17.68	Top nozzle	SS 304	8.346
		Hold-down spring	Inconel-718	1.2
GP	26.07	Spacer (plenum)	Inconel-718	0.77
Active Fuel	347.22	Spacer (in core)	Inconel-718	6.759
		Grid sleeves	SS 304	0.658
		Guide tubes	Zircaloy-4	10.95
LEF	7.94	Bottom nozzle	SS 304	5.44

Table 11. Fuel assembly hardware dimensions and materials for the C1616CSD assembly.

Axial fuel assembly zone	Length (cm)	Assembly parts in the zone	Material	Weight (kg/assembly)
UEF	30.03	Hold-down spring	CE Ni Alloy	4.5
		Locking posts	SS 304	7.3
		Flow plate	SS 304	3.2
		Hold-down plate	SS 304	1.8
GP	26.10	Spacer (plenum)	Zircaloy-4	0.82
Active Fuel	381	Guide tubes	Zircaloy-4	10.9
		Spacer (in core)	Zircaloy-4	7.35
		Spacer (lower)	Inconel-625	1.36
LEF	11.95	Bottom nozzle	SS 304	5.4

Table 12. Fuel assembly hardware dimensions and materials for the W1414WL assembly.

Axial fuel assembly zone	Length (cm)	Assembly parts in the zone	Material	Weight (kg/assembly)
UEF	12.554	Top nozzle	SS 304	9.38
		Hold-down spring	Inconel-718	0.508
GP	15.088	Spacer (plenum)	Inconel-718	0.612
			West. Braze	0.068
Active Fuel	365.76	Spacer (in core)	Inconel-718	5.37
		Guide tubes	Zircaloy-4	7.98
LEF	12.49	Bottom nozzle	SS 304	7.893

Table 13. Fuel assembly hardware dimensions and materials for the W1515WL assembly.

Axial fuel assembly zone	Length (cm)	Assembly parts in the zone	Material	Weight (kg/assembly)
UEF	11.92	Top nozzle	SS 304	10.7
		Hold-down spring	Inconel-718	1.14
GP	18.13	Spacer (plenum)	Inconel-718	0.7344
			West. Braze	0.0816
		Grid sleeve	SS 304	0.25
Active Fuel	365.76	Spacer (in core)	Inconel-718	6.8
		Guide tubes	Zircaloy-4	9.39
		Grid sleeves	SS 304	1.25
LEF	10.00	Bottom nozzle	SS 304	5.44

Table 14. Fuel assembly hardware dimensions and materials for the W1717WL assembly.

Axial fuel assembly zone	Length (cm)	Assembly parts in the zone	Material	Weight (kg/assembly)
UEF	13.44	Hold-down spring	Inconel-718	0.96
		Top nozzle	SS 304	6.89
GP	14.66	Spacer (plenum)	Inconel-718	0.7137
			West. Braze	0.0793
		Grid sleeve	SS 304	0.091
Active Fuel	365.76	Spacer (in core)	Inconel-718	4.9
		Guide tubes	Zircaloy-4	9.526
		Grid sleeves	SS 304	0.54
LEF	11.95	Bottom nozzle	SS 304	5.9

Table 15. Fuel assembly hardware dimensions and materials for the W1717WO assembly.

Axial fuel assembly zone	Length (cm)	Assembly parts in the zone	Material	Weight (kg/assembly)
UEF	12.44	Top nozzle	SS 304	6.89
		Hold-down spring	Inconel-718	0.96
GP	17.53	Spacer (plenum)	Inconel-718	0.7965
			West. Braze	0.0885
		Grid sleeve	SS 304	0.091
Active Fuel	365.76	Spacer (lower)	Inconel-718	0.925
		Spacer (in core)	Zircaloy-4	7.022
		Guide tubes	Zircaloy-4	9.53
		B. Grid sleeve	SS 304	0.091
LEF	10.08	Bottom nozzle	SS 304	5.897

Table 16. Fuel assembly hardware dimensions and materials for the Haddam Neck XHN15B, XHN15WZ, and XHN15BZ assemblies.

Axial fuel assembly zone	Length [a] (cm)	Assembly parts in the zone [a]	Material [a]	Weight [a] (kg/assembly)
UEF	19.56	Top nozzle	SS CF3M	9.48
		Hold-down spring	Inconel-718	0.33
		Upper nut	SS 304	0.13
GP	12.67	Spacer (plenum)	Inconel-718	0.64
Active Fuel	306.07	Guide tubes	SS 304	7.26
		Instrument tube	SS 304	0.35
		Spacer (in core)	Inconel-718	3.8
LEF	9.84	Bottom nozzle	SS 304L	6.3
		Lower nut	SS 304	0.08

[a] Data for the Haddam Neck XHN15B, XHN15BZ, and XHN15WZ assemblies were not available. The data for the B&W 15 × 15 stainless-steel PWR assembly design [2] are assumed instead because all these assemblies have the same active fuel length.

Table 17. Fuel assembly hardware dimensions and materials for the XHN15W assembly.

Axial fuel assembly zone	Length (cm)	Assembly parts in the zone	Material	Weight (kg/assembly)
UEF	19.30	Top nozzle	SS 304	10.7
		Hold-down spring	SS 304	0.54
GP	11.41	Spacer (plenum)	Inconel-718	0.7794
			West. Braze	0.0866
Active Fuel	309.372	Spacer (in core)	Inconel-718	5.198
		Guide tubes	SS 304	7.26
LEF	8.04	Bottom nozzle	SS 304	8.85

Table 18. Fuel assembly hardware dimensions and materials for the XPA15C assembly.

Axial fuel assembly zone	Length (cm)	Assembly parts in the zone	Material	Weight (kg/assembly)
UEF	7.97	Top nozzle	SS 304	4.5
GP	23.17	Spacer (plenum)	Zircaloy-4	0.81
Active Fuel	335.28	Spacer (in core)	Zircaloy-4	6.45
		Guide bars	Zircaloy-4	21.3
		Spacer (lower)	Inconel-625	0.82
		Instrument tube	Zircaloy-4	0.45
LEF	8.23	Bottom nozzle	SS 304	5.4

Table 19. Fuel assembly hardware dimensions and materials for the XSO14W assembly.

Axial fuel assembly zone	Length (cm)	Assembly parts in the zone	Material	Weight (kg/assembly)
UEF	19.74	Top nozzle	SS 304	9.21
		Hold-down spring	Inconel-718	0.41
GP	15.50	Spacer (plenum)	Inconel-718	0.671
Active Fuel	304.8	Spacer (in core)	Inconel-718	3.48
		Guide tubes	SS 304	7.185
LEF	8.10	Bottom nozzle	SS 304	7.89

Table 20. Fuel assembly hardware dimensions and materials for the Yankee Rowe XYR16C assembly.

Axial fuel assembly zone	Length (cm)	Assembly parts in the zone	Material	Weight (kg/assembly)
UEF	23.561	Top nozzle	SS 304	8.2
GP	5.817	Spacer (plenum)	Zircaloy-4	0.64
Active Fuel	231.14	Spacer (in core)	Zircaloy-4	2.5
		Spacer (lower)	Inconel-625	0.91
		Guide bars	Zircaloy-4	13.2
		Instrument tube	Zircaloy-4	0.45
LEF	23.622	Bottom nozzle	SS 304	9.1

2.2 BWR FUEL ASSEMBLIES

Section 2.2.1 presents data for the active fuel region, and Section 2.2.2 provides data for the fuel assembly hardware of the main BWR/4-6 fuel assembly classes.

2.2.1 BWR Fuel Region Characteristics

Fuel region characteristics for the BWR/4-6 fuel assembly classes are provided in Table 21, and these characteristics for assembly classes Big Rock Point (XBR09A), Dresden-1 (XDR06G5), and LaCrosse (XLC10A) are provided in Table 22.

Table 21. Fuel region characteristics for the BWR/4–6 fuel class.

GC-859 assembly type code (Fuel design)	G4607G3B (7×7 GE-3b)	G4608G4B (8×8 GE-4b)	G4609A (9×9 ANF)	G4610G14 (10×10 GE14)	G4610A (Atrium-10)
Array size	7 × 7	8 × 8	9 × 9	10 × 10	10 × 10
Initial ^{235}U enrichment mean (wt %)	2.31	2.40	3.42	4.03	3.93
Initial ^{235}U enrichment range (wt %)	1.09–2.51	2.17–2.76	0.72–3.73	1.47–4.43	1.63–4.26
Average initial U mass (kg)	189.93	186.82	172.55	179.25	177.70
Initial U range (kg)	188.45–191.54	185.87–187.89	172.29–175.66	173.67–183.37	175.15–179.70
Active fuel rod length (cm)	370.44	370.84	381	381	378.46
Number of fuel rods	49	63	79	92	91
Rod pitch (cm)	1.87452	1.6256	1.45228	1.295	1.2954
Clad material	Zircaloy-2	Zircaloy-2	Zircaloy-2	Zircaloy-2	Zircaloy-2
Clad OD (cm)	1.43002	1.25222	1.07696	1.026	1.005078
Clad thickness (cm)	0.09398	0.08636	0.0762	0.066	0.06096
Fuel pellet diameter (cm)	1.21158	1.05664	0.88456	0.876	0.866902
Number of water rods	0	1	0	2	1
Water rod material	N/A	Zircaloy-4	N/A	Zircaloy-2	Zircaloy-4
Water rod OD (cm)	N/A	1.25222	N/A	2.522	3.50012
Water rod ID (cm)	N/A	1.0795	N/A	2.322	3.35534

Table 22. Fuel region characteristics for assembly classes Big Rock Point (XBR09A), Dresden-1 (XDR06G5), and LaCrosse (XLC10A).

GC-859 assembly type code (Fuel design)	XBR09A (Big Rock Point 9 × 9 ANF)	XDR06G5 (Dresden-1 6 × 6 GE Type 5)	XLC10A (LaCrosse 10 × 10 AC)
Array size	9 × 9	6 × 6	10 × 10
Initial ^{235}U enrichment mean (wt %)	3.48	2.26	3.69
Initial ^{235}U enrichment range (wt %)	3.45–3.52	2.26–2.26	3.68–3.71
Average initial U mass (kg)	127.69	105.86	108.66
Initial U range (kg)	123.98–131.41	104.72–112.26	107.51–109.61
Active fuel rod length (cm)	172.72	274.955	210.82
Number of fuel rods	77	36	96
Rod pitch (cm)	1.79578	1.8034	1.41478
Clad material	Zircaloy-2	Zircaloy-2	SS348H
Clad OD (cm)	1.42875	1.42875	1.00076
Clad thickness (cm)	0.08636	0.0889	0.05588
Fuel pellet diameter (cm)	1.21603	1.22428	0.889
Number of water rods	0	0	0
Water rod material	N/A	N/A	N/A
Water rod OD (cm)	N/A	N/A	N/A
Water rod ID (cm)	N/A	N/A	N/A

2.2.1.1 Part-Length Fuel Rods

Modern BWR fuel assemblies contain a limited number of partial-length fuel rods that extend from the lower tie plate to an intermediate level below the upper tie plate. Typically, 14 partial length fuel rods are provided for a General Electric (GE)-14 fuel bundle [16]. The length of the part length fuel rods could vary, and the nominal active fuel length of the GE-14 part-length fuel rods is 213.36 cm [17]. This fuel design mitigates the loss of shutdown margin caused by increased ^{239}Pu production associated with the steam environment in the upper part of a BWR operating core.

2.2.2 BWR Fuel Assembly Hardware

This section presents the characteristics of NFH regions of the assembly types G4607G3B (Table 23), G4608G4B (Table 24), G4609A (Table 25), Dresden-1 XDR06G5 (Table 26), and LaCrosse XLC10A (Table 27). No data were available for the assembly types G4610G14, Big Rock Point XBR09A, and G4610A.

Table 23. Fuel assembly hardware dimensions and materials for the G4607G3B assembly.

Axial fuel assembly zone	Length (cm)	Assembly parts in the zone	Material	Weight (kg/assembly)
UEF	22.39	Compression springs [a]	Inconel X-750	0
		Top tie plate	SS 304	1.915
GP	35.44	–	–	–
Active Fuel	370.44	Spacers	Zircaloy-4	2.029
			Inconel X-750	
LEF	19.18	Bottom tie plate	SS 304	4.408

[a] The tie plate mass might include the compression springs for this assembly.

Table 24. Fuel assembly hardware dimensions and materials for the G4608G4B assembly.

Axial fuel assembly zone	Length (cm)	Assembly parts in the zone	Material	Weight (kg/assembly)
UEF	23.62	Compression springs [a]	Inconel X-750	0
		Top tie plate	SS 304	2
GP	34.23	–	–	–
Active Fuel	370.84	Spacers	Zircaloy-4	2.275
			Inconel X-750	
		Water rod	Zircaloy-2	0.87
LEF	18.76	Bottom tie plate	SS 304	4.831

[a] The tie plate mass might include the compression springs for this assembly.

Table 25. Fuel assembly hardware dimensions and materials for the G4609A assembly.

Axial fuel assembly zone	Length (cm)	Assembly parts in the zone	Material	Weight (kg/assembly)
UEF	23.84	Compression springs	Inconel X-750	0.34
		Top tie plate	SS-ANF	1.61
GP	24.33	–	–	–
Active Fuel	381	Spacer (in core)	Zircaloy-4	1.2936
			Inconel-718	0.2464
		Inert rod	Zircaloy-2	0.65
		Spacer capture rod	Zircaloy-2	0.65
LEF	18.02	Bottom tie plate	SS-ANF	4.53

Table 26. Fuel assembly hardware dimensions and materials for the XDR06G5 assembly.

Axial fuel assembly zone	Length (cm)	Assembly parts in the zone	Material	Weight (kg/assembly)
UEF	22.098 [a]	Top tie plate	SS-ANF	1.55
		Compression springs	Inconel X-750	0.11
GP	13.3858	–	–	–
Active Fuel	274.955	Spacer (in core)	Zircaloy-4	0.9324
			Inconel-718	0.1776
		Inert rod	Zircaloy-2	0.94
LEF	22.098 [a]	Bottom tie plate	SS-ANF	5.73

[a] Assumed (i.e., not available).

Table 27. Fuel assembly hardware dimensions and materials for the XLC10A assembly.

Axial fuel assembly zone	Length (cm)	Assembly parts in the zone	Material	Weight (kg/assembly)
UEF	9.55	Compression springs	Inconel X-750	0.11
		Top tie plate	SS-ANF	1.24
GP	9.8806	–	–	–
Active Fuel	210.82	Spacer (in core)	SS-ANF	0.5002
			Zircaloy-4	0.1098
		Inert rod	SS-ANF	3.234
			Inconel X-750	0.066
		Spacer capture rod	SS-ANF	1.100358
			Inconel X-750	0.006642
LEF	24.4	Bottom tie plate	SS-ANF	10.46

2.3 LIGHT ELEMENT IMPURITIES IN UO_2 MATRIX

In UO_2 fuel, $^{17}O(\alpha,n)^{20}Ne$ and $^{18}O(\alpha,n)^{21}Ne$ reactions are the principal source of neutrons from (α,n) reactions because of the large amount of O compared with other light elements that might be present in the fuel. NUREG/CR-6802 [26] indicates that for situations in which the (α,n) contribution to the total neutron source is significant, it is necessary to accurately quantify or establish bounding values for all impurities, especially light elements that are known to produce significant (α,n) quantities. In irradiated nuclear fuels that achieve a moderate to high burnup, the neutron source is typically dominated by $^{242,244}Cm$ spontaneous fission, but the (α,n) neutron processes can represent a larger component of the total neutron source in low-burnup fuels [27]. Light nuclei—such as $^{6,7}Li$, ^{9}Be, $^{10,11}B$, $^{12,13}C$, $^{14,15}N$, and $^{17,18}O$—have large cross sections for neutron production [28, 29]. This section provides publicly available information on impurity concentration levels in LWR fuel and an evaluation of impurity effects on the neutron source from (α,n) reactions relative to pure UO_2.

Maximum concentration limits are imposed on certain impurity elements in UF_6 (ASTM C996 [30], ASTM C787 [31]); nuclear-grade, sinterable UO_2 powder (ASTM-C753 [32]); nuclear-grade gadolinium oxide powder (ASTM-C888 [33]); UO_2 pellets for LWRs (ASTM-C776 [34]); and Gd_2O_3–UO_2 pellets (ASTM-C922 [35]). Impurity limits for B (4 μg/gU) and Si (250 μg/gU) in UF_6 enriched to less than 5% ^{235}U are specified in ASTM-C996. The impurity limits specified in ASTM-C776, ASTM-C922, ASTM-C753, and ASTM-C888 are provided in Table 28. ASTM-C753 indicates that additional impurity elements might be present in UO_2 powder, but no limits are provided for those elements. However, the equivalent B content (EBC) [36] for thermal reactor use shall not exceed 4 μg/gU [34]. For the purpose of EBC calculation, B, Gd, Eu, Dy, Sm, and Cd shall be included in addition to the impurity elements listed in ASTM-C776 [34]. Concerning stoichiometry, the O to U ratio of sintered fuel pellets is limited to 1.99–2.02 [34].

Table 28. Fuel impurities and maximum elemental concentration limits as specified in ASTM standards.

UO_2 (ASTM-C776) and Gd_2O_3 pellets (ASTM-C922)		UO_2 powder (ASTM-C753)		Gd_2O_3 powder (ASTM-C888)	
Element	**Maximum concentration limit (µg/gU)**	**Element**	**Maximum concentration limit (µg/gU)**	**Element**	**Maximum concentration limit (µg/g Gd_2O_3)**
Al	250	Al	300	B	5
C	100	C	100	Cd	25
Ca + Mg	200	Ca + Mg	200	Th	30
Cl	25	Cl	100	Cl + F	100
Cr	250	Cr	200	Eu + Sm + Tb + Yb + Dy	1,000
Co	100	Co	100	C	600
F	15	Cu	250	–	–
H	1.3	F	100	–	–
Fe	500	Fe	250	–	–
Ni	250	Pb	250	–	–
N	75	Mn	250	–	–
Si	500	Mo	250	–	–
Th	10	Ni	200	–	–
–	–	N	200	–	–
–	–	P	250	–	–
–	–	Si	300	–	–
–	–	Ta	250	–	–
–	–	Th	10	–	–
–	–	Sn	250	–	–
–	–	Ti	250	–	–
–	–	W	250	–	–
–	–	V	250	–	–
–	–	Zn	250	–	–

Actual fuel impurity concentration measurements are not readily available. Measuring trace elements in two UO_2 pellets [37] showed that all but W impurities were below the accepted impurity values for UF_6 prepared for enrichment, and Li and Be were below the detection limits. The levels of elemental impurities in LWR fuel were estimated in the VTT-R-00184-20 report [38] based on a literature survey. The maximum concentration values of light elements (i.e., elements with an atomic number of less than 20) in UO_2 from that report are shown in Table 29, along with light element concentration in LWR oxide fuel from the ORNL-TM-6051 report [39]. The light element impurity concentrations from the VTT-R-00184-20 report [38] are most limiting among all sources of information mentioned here. The effects of light element impurities on the neutron source from (α,n) reactions are evaluated in this report by using SCALE/ORIGAMI [40] calculations for B&W 15 × 15 fuel assemblies and the ORIGEN cross section libraries available in SCALE for this fuel assembly type. These effects were evaluated as a function of burnup (40–60 GWd/MTU) and cooling time (5–40 years). As shown in Table 30, the neutron source strength from (α,n) reactions increased by approximately 18% when adding light element

impurities to the pure UO_2 composition. However, this increase did not significantly raise the total neutron strength of the fuel assembly because the contribution of the neutron source from (α,n) reactions to the total neutron source strength is relatively small (i.e., ~ 1% for the evaluated cases).

Table 29. Light element impurities plus Co in LWR oxide fuel.

Element	**Maximum concentration limit (μg/gU)** [38]	**Element**	**Concentration (μg/gU)** [39]
H	1	Li	1.0
Li	1	B	1.0
Be	0.1	C	89.4
B	1	N	25.0
C	200	F	10.7
N	200	Na	15.0
F	50	Mg	2.0
Na	400	Al	16.7
Mg	200	Si	12.1
Al	400	P	35.0
Si	250	Cl	5.3
P	60	Ca	2.0
S	20	Co	1.0
Cl	15		
K	20		
Ca	250		
Co	75		

Table 30. Effects of light element impurities on the neutron sources from (α,n) reactions as a function of assembly average burnup and cooling time for a B&W 15 × 15 fuel assembly.

			Pure UO_2			UO_2 + light element impurities			Ratio [e]		
Burnup [a] (GWd/MTU)	E [b] (wt%)	CT [c] (years)	(α,n)	SF [d]	Total	(α,n)	SF [d]	Total	(α,n)	SF [d]	Total
20	2.5	5	9.90E+05	2.30E+07	2.40E+07	1.15E+06	2.30E+07	2.42E+07	1.16	1.00	1.01
30	2.9	5	2.33E+06	1.13E+08	1.15E+08	2.73E+06	1.13E+08	1.16E+08	1.17	1.00	1.00
40	3.2	5	4.60E+06	3.07E+08	3.12E+08	5.42E+06	3.07E+08	3.12E+08	1.18	1.00	1.00
40	3.2	10	4.48E+06	2.54E+08	2.59E+08	5.27E+06	2.54E+08	2.59E+08	1.18	1.00	1.00
40	3.2	20	4.26E+06	1.75E+08	1.79E+08	5.00E+06	1.75E+08	1.80E+08	1.17	1.00	1.00
40	3.2	40	3.83E+06	8.38E+07	8.77E+07	4.47E+06	8.38E+07	8.83E+07	1.17	1.00	1.01
50	3.8	5	7.41E+06	5.61E+08	5.69E+08	8.75E+06	5.61E+08	5.70E+08	1.18	1.00	1.00
50	3.8	10	6.99E+06	4.64E+08	4.71E+08	8.24E+06	4.64E+08	4.72E+08	1.18	1.00	1.00
50	3.8	20	6.30E+06	3.19E+08	3.26E+08	7.40E+06	3.19E+08	3.27E+08	1.17	1.00	1.00
50	3.8	40	5.28E+06	1.53E+08	1.59E+08	6.17E+06	1.53E+08	1.60E+08	1.17	1.00	1.01
60	4.2	5	1.13E+07	9.56E+08	9.68E+08	1.34E+07	9.56E+08	9.70E+08	1.18	1.00	1.00
60	4.2	10	1.04E+07	7.89E+08	7.99E+08	1.23E+07	7.89E+08	8.01E+08	1.18	1.00	1.00
60	4.2	20	8.98E+06	5.43E+08	5.52E+08	1.06E+07	5.43E+08	5.53E+08	1.18	1.00	1.00
60	4.2	40	7.03E+06	2.62E+08	2.69E+08	8.23E+06	2.62E+08	2.70E+08	1.17	1.00	1.00

[a] Assembly average burnup (GWd/MTU).
[b] Fuel initial enrichment (^{235}U wt %).
[c] Cooling time (years).
[d] Neutron source strength from spontaneous fission.
[e] Ratio between neutron source strength in UO_2 fuel containing light element impurities to neutron source strength in pure UO_2 fuel.

2.4 ENRICHMENT ZONING AND INTEGRAL NEUTRON ABSORBER

Axial and radial enrichment zoning are routinely used in modern BWR fuel assemblies [16]. Integral burnable absorbers (e.g., Gd_2O_3) are used in both BWR and PWR fuel assemblies. Gadolinia-bearing (Gd_2O_3-UO_2) fuel rods have lower ^{235}U initial enrichment because gadolinia reduces the thermal conductivity. Actual enrichment/integral absorption zoning data are proprietary and therefore unavailable. However, a few examples of representative assembly enrichment zoning are available (e.g., *General Electric Systems Technology Manual* [16]).

2.5 AXIAL BLANKET REGIONS

An axial blanket fuel design was introduced to decrease axial leakage and increase discharge burnup in the enriched fuel relative to non-blanketed fuel. This design change implemented in both PWR and BWR fuel assemblies provides improved U utilization and reduced fuel cycle costs. A previous axial blanket demonstration program [21] conducted in 1980 showed that the most economical option for the U enrichment in the blanket regions is natural U. Typically, the top and bottom 6 in. of enriched U in a fuel rod are replaced with natural U in blanketed fuel, but a fuel assembly might contain fuel rods with longer blanketed fuel regions and higher enrichment [41, 42]. WE integral fuel burnable absorber (IFBA) fuel rods (e.g., UO_2 with ZrB_2 coating) contain annular blanket regions, which provide additional volume for fission gases and He generated by IFBA depletion.

2.6 ANTICIPATED INCREASE IN FUEL ENRICHMENT/BURNUP

The nuclear industry is considering a transition within the next decade to extended fuel burnup (peak rod average burnup >62 GWd/MTU) and higher fuel enrichment (^{235}U > 5 wt %) as described in a white paper titled *The Economic Benefit and Challenges with Utilizing Increased Enrichment and Fuel Burnup for Light-Water Reactors*, published by the Nuclear Energy Institute (NEI) [43]. Fuel cycle economics studies for PWRs and BWRs conducted by the Electric Power Research Institute [41, 42] showed that peak rod burnups could be increased to ~75 GWd/MTU by increasing the fuel rod enrichment up to ~6%. However, fuel mechanical and nuclear design changes would be required to mitigate high burnup phenomena, such as increases in rod internal pressure, cladding corrosion, rod and assembly growth, fuel fragmentation, and cladding strain. A greater amount of thermal neutron absorbers would also be required to balance the higher reactivity cores associated with higher initial enrichments. For PWRs, additional burnable poisons in the fuel could control core reactivity during initial operations, and an increase in the amount of ^{10}B in the cooling water could control the reactivity thereafter [59]. Peak rod burnup values between 75 and 80 GWd/MTU would require fuel enrichments from 10 to 20% and future fuel concepts and designs [43].

The NEI white paper indicates that the industry has already made progress toward developing new technologies that enable extended enrichment and/or burnup for LWRs. Examples include the ongoing accident-tolerant fuel (ATF) and high-assay low-enriched uranium programs [44]. ATF features are designed to improve fuel system performance under accident conditions. The ATF concepts include oxide-doped UO_2, barrier cladding materials (i.e., Zr-alloy liner), new cladding materials (e.g., FeCrAl and SiC), and high-density fuel (e.g., high-density uranium silicide and nitride fuels). High-density fuel could be developed as an alternative to higher enrichment because higher U density has a similar effect to increasing ^{235}U enrichment in UO_2 fuels. Of these concepts, oxide-doped UO_2 and barrier and steel cladding materials are considered to be near-term technologies with respect to the time of commercial deployment [44].

Various dopants have been used to increase the grain size in UO_2 (e.g., TiO_2, Nb_2O_5, Cr_2O_3) in which the content of metals in U varies from 0.05 to 1 wt % [45]. AREVA has developed chromia-doped fuel by adding a small amount of Cr_2O_3 (<5,000 ppm) to the standard fuel for PWRs and BWRs [20]. WE has developed Advanced Doped Pellet Technology UO_2 fuel that contains additions of Cr and Al oxides on the order of 1,000 ppm and 200 ppm, respectively [46]. Doped fuel has a larger grain size than standard fuel because the added dopants enhance grain grows during sintering. The typical thickness of the Zr-alloy liner is on the order of 60–80 μm [47]. The Zr-liner could be a sponge Zr-liner or an Fe-alloy liner. The Fe concentration in the Fe-liner is on the order of a few thousands parts per million (e.g., 4,000 ppm) [47]. More relevant information is summarized in the ORNL/TM-2021/1961 report [48].

New materials for an accident-tolerant control rod (ATCR) are also evaluated. Current neutron absorber materials used in control rods include B_4C and Hf metal in BWRs and Ag-In-Cd alloy in PWRs. These materials cannot prevent control rod breakage before extensive fuel rod failure caused by severe accidents. Candidate new absorber materials for ATCR include neutron absorber materials with a high melting point and high eutectic temperature with cladding, such as Gd_2O_3, Sm_2O_3, Eu_2O_3, Dy_2O_3, and HfO_2 [49].

3. NUCLEAR FUEL OPERATING CONDITIONS

This section provides information on representative nuclear fuel operating conditions for PWR (Section 3.1) and BWR (Section 3.2) fuel assemblies, as well as information on solid stainless-steel filler rods (Section 3.3).

3.1 PWR FUEL ASSEMBLIES

3.1.1 PWR Moderator Density and Fuel Temperature

Cycle-averaged moderator density and fuel temperature values for McGuire Unit 1, cycles 2–7, [7] are provided in Table 31. McGuire Unit 1 is a representative WE four-loop PWR that used WE 17 × 17 fuel assemblies, except for cycles 5–7, which also used B&W 17 × 17 fuel assemblies (~10% of the core).

Table 31. Cycle-averaged moderator density and fuel temperature for McGuire fuel.

	Cycle 2	Cycle 3	Cycle 4	Cycle 5	Cycle 6	Cycle 7
Moderator density (g/cm^3)						
Min	0.643	0.649	0.631	0.631	0.633	0.631
Max	0.742	0.742	0.742	0.742	0.742	0.742
Mean	0.703	0.710	0.701	0.700	0.703	0.702
Median	0.707	0.715	0.703	0.703	0.709	0.706
10%	0.663	0.677	0.656	0.656	0.661	0.659
25%	0.690	0.696	0.682	0.679	0.682	0.681
75%	0.726	0.729	0.725	0.725	0.728	0.725
90%	0.735	0.738	0.735	0.735	0.738	0.735
Fuel temperature (K)						
Min	797.40	689.30	656.30	638.00	645.80	651.80
Max	1,218.80	1,237.20	1,343.30	1,346.80	1,430.50	1,382.60
Mean	1,058.19	957.64	1,066.50	1,058.20	1,018.33	1,012.67
Median	976.30	940.30	1,096.35	1,084.05	1,006.75	992.50
10%	930.69	774.52	864.91	841.20	754.20	792.99
25%	969.28	793.20	948.60	901.98	863.53	893.85
75%	1,204.33	1,143.75	1,181.00	1,183.20	1,162.53	1,131.08
90%	1,211.97	1,231.97	1,290.42	1,283.70	1,302.57	1,242.35

3.1.2 Boron Letdown Curve Data

The two-cycle B letdown values available in BEAVRS (Benchmark for Evaluation of Reactor Simulations) [50] based on measurement data from a four-loop WE power reactor are presented in Table 32. These data provide soluble B concentration (ppm) in reactor primary coolant as a function of effective full-power days (EFPDs) for cycles 1 and 2.

Table 32. B letdown curve data for PWR cycles 1 and 2.

Cycle 1		Cycle 2	
EFPD	**B (ppm)**	**EFPD**	**B (ppm)**
4	599	13	918
11	610	23	882
16	614	43	832
22	621	63	764
31	638	84	687
36	610	103	623
52	623	129	538
69	598	150	466
85	569	176	376
96	559	202	292
110	533	234	184
124	506	257	104
141	471		
144	461		
152	457		
164	415		
174	394		
177	384		
180	384		
190	367		
204	322		
214	296		
219	286		
225	270		
228	270		
248	207		
271	149		
295	72		
326	0		

Extended fuel burnup and longer fuel cycles require higher soluble B concentrations at the beginning of cycles. Soluble B concentrations up to 2,000 ppm and cycle lengths of up to 690 days are analyzed in the Electric Power Research Institute report TR-105714-V1R4 [51]. The McGuire Unit 1 and Crystal River Unit 3 CRC data [7, 8] confirm this trend, as shown in Table 33 and Table 34, respectively. Because the soluble B concentration in water typically decreases linearly as a function of EFPD, a formula can be used to calculate critical boron data for McGuire Unit 1, cycles 2–7 [7]:

$$\text{ppm} = A + B \times \text{EFPD},$$

where the A and B coefficients are provided in Table 33 as a function of cycle.

Table 33. Critical B data for McGuire Unit 1 cycles 2–7.

Cycle	EFPD	A (ppmB) [a]	B (ppmB/EFPD)
2 [b]	268.0	877.99	-3.57
3 [c]	288.5	904.82	-3.21
4	300.0	1018.04	-3.39
5	316.3	1116.42	-3.38
6	298.0	1159.67	-3.02
7	408.0	1363.64	-3.08

[a] *ppmB* stands for *parts per million boron.*
[b] For cycle 2, use the equation out to 243.1 EFPD and 10 ppm from 243.1 EFPD to end-of-cycle.
[c] For cycle 2, use the equation out to 287.7 EFPD and 10 ppm from 287.7 EFPD to end-of-cycle.

Table 34. B letdown data for Crystal River Unit 3 cycles 6–10.

Cycle 6		Cycle 7		Cycle 8		Cycle 9		Cycle 10	
EFPD	ppmB [a]	EFPD	ppmB	EFPD	ppmB	EFPD	ppmB	EFPD	ppmB
9.20	1017	7.50	1478	11.20	1537	22.10	1608	4.00	1752
22.30	1012	41.40	1405	52.40	1455	61.50	1535	27.30	1712
49.80	995	60.30	1367	78.00	1411	145.70	1329	48.30	1660
68.50	952	81.70	1333	111.40	1332	192.80	1201	76.10	1612
84.60	908	102.90	1290	154.40	1176	211.30	1157	104.50	1547
127.30	778	122.30	1245	194.80	1103	262.00	994	124.80	1497
140.10	727	139.80	1204	234.60	999	303.70	869	152.70	1422
184.50	631	160.50	1167	271.50	887	345.70	750	174.00	1333
202.80	567	180.80	1102	338.00	701	397.90	577	199.80	1259
248.80	441	202.80	1040	390.70	522	432.50	473	227.90	1183
274.90	366	230.90	963	445.70	394	452.40	412	248.70	1124
288.20	337	251.20	898	474.00	311	495.40	283	276.70	1040
318.20	266	306.70	803	513.10	216	543.40	136	297.10	985
331.60	229	317.90	775					326.40	896
349.70	183	345.30	593					347.60	830
367.40	139	412.30	398					370.60	766
373.30	123	459.80	260					403.20	652
393.30	156	485.00	193					431.90	555
397.70	137							450.40	498
405.30	123							470.70	436
								504.90	302
								525.50	239
								560.50	155
								573.70	120
								591.70	72

3.1.3 PWR Average Assembly Burnup and Specific Power

Mean values and the range of values for assembly average burnup and specific power obtained from the 2013 CG-859 survey data are provided for fuel assemblies in the assembly classes B&W 15 × 15 (Table 35); CE 14 × 14 and 16 × 16 (Table 36); WE 14 × 14, 15 × 15, and 17 × 17 (Table 37); and site-specific assembly classes Haddam Neck (Table 38), Indian Point-1, Palisades, San Onofre-1, and Yankee Rowe (Table 39). The 2013 CG-859 survey data indicate several discharged BWR and PWR fuel assemblies with average burnup greater than 65 GWd/MTU. The outlier data are considered errors in the database [15].

Table 35. Assembly average burnup and specific power for the B&W 15 × 15 assembly class.

GC-859 assembly type code	B1515B3	B1515B4	B1515B4Z	B1515B8	B1515B9	B1515B10
Burnup mean (MWd/MTU)	21,175	34,717	39,253	42,831	44,131	45,363
Burnup range (MWd/MTU)	8,652–3,2267	10,809–58,160	33,119–51,660	27,124–54,000	16,526–53,952	33,553–56,880
Specific power mean (MW/MTU)	22.05	25.68	23.89	29.91	31.30	30.44
Specific power range (MW/MTU)	17.29–26.02	9.80–51.43	17.16–31.20	19.60–44.61	17.88–41.26	17.56–43.11

Table 36. Assembly average burnup and specific power for assembly classes CE 14 × 14 and 16 × 16.

GC-859 assembly type code	C1414A	C1414C	C1414W	C1616CSD
Burnup mean (MWd/MTU)	42,249	33,819	40,837	38,788
Burnup range (MWd/MTU)	2,397–62,611	2,768–57,165	7,339–62,788	11,680–63,328
Specific power mean (MW/MTU)	28.59	26.76	29.42	33.82
Specific power range (MW/MTU)	2.50–41.91	10.12–39.05	15.64–40.89	18.48–46.89

Table 37. Assembly average burnup and specific power for assembly classes WE 14 × 14, 15 × 15, and 17 × 17.

GC-859 assembly type code	W1414WL	W1515WL	W1717WL	W1717WO
Burnup mean (MWd/MTU)	37,764	37,071	44,116	50,768
Burnup range (MWd/MTU)	10,774–59,224 [a]	2,971–58,598	11,810–58,417 [a]	44,578–58,237
Specific power mean (MW/MTU)	30.55	28.76	40.58	44.02
Specific power range (MW/MTU)	15.89–54.67	4.41–44.68	11.86–54.97	29.55–52.22

[a]After removing outlier values.

Table 38. Assembly average burnup and specific power for the Haddam Neck assembly class.

GC-859 assembly type code	XHN15B	XHN15BZ	XHN15W	XHN15WZ
Burnup mean (MWd/MTU)	33,776	34,278	27,922	14,321
Burnup range (MWd/MTU)	8,193–37,833	23,813–42,956	10,742–35,196	8,874–19,376
Specific power mean (MW/MTU)	25.66	27.86	22.63	31.13
Specific power range (MW/MTU)	17.36–29.97	23.41–30.55	10.76–28.44	19.29–42.12

Table 39. Assembly average burnup and specific power for site-specific assembly classes Indian Point-1 (XIP14W), Palisades (XPA15C), San Onofre-1 (XSO14W), and Yankee Rowe (XYR16C).

GC-859 assembly type code	XIP14W	XPA15C	XSO14W	XYR16C
Burnup mean (MWd/MTU)	16,471	16,020	27,232	24,282
Burnup range (MWd/MTU)	3,704–27,048	5,139–33,630	6,800–39,275	6,039–35,999
Specific power mean (MW/MTU)	13.95	13.24	17.20	30.36
Specific power range (MW/MTU)	7.91–22.31	6.12–24.02	8.90–29.17	18.70–37.41

3.2 BWR FUEL ASSEMBLIES

3.2.1 BWR Moderator Density and Fuel Temperature

BWR moderator density range and nominal moderator density were provided in the Framatome ANP report 32–5030781–00 [52] based on Grand Gulf Unit 1 thermal-hydraulic data. The nominal moderator density was 0.43 g/cm^3, and the moderator density range was 0.12–0.74 g/cm^3 in that report. The range for the average moderator density indicated in the LSCS-UFSAR report [17] is 0.415–0.428 g/cm^3. Cycle-averaged moderator density and fuel temperature values for LaSalle Unit 1 cycles 4–8 [8] are provided in Table 40. LaSalle Unit 1 is a representative GE Type 5 BWR. The reference moderator density (zero void fraction) for the core nominal operating pressure provided in the CRC reports is 0.7396 g/cm^3 [9].

A similar range (i.e., 0.243–0.754 g/cm^3) and average value (0.444 g/cm^3) are provided in NUREG/CR-6802 [26]. However, the study in NUREG/CR-7224 [53] identified a minimum moderator density of 0.107 g/cm^3 based on a set of data representative of more modern BWR operating regimes.

Table 40. Cycle-averaged moderator density and fuel temperature for LaSalle Unit 1 fuel.

	Cycle 4	Cycle 5	Cycle 6	Cycle 7	Cycle 8
Moderator density (g/cm^3)					
Min	0.188	0.177	0.176	0.174	0.181
Max	0.74	0.74	0.74	0.74	0.74
Mean	0.397	0.39	0.388	0.399	0.408
Median	0.319	0.315	0.317	0.332	0.344
10%	0.224	0.206	0.205	0.216	0.218
25%	0.247	0.233	0.235	0.247	0.253
75%	0.531	0.53	0.515	0.534	0.549
90%	0.735	0.729	0.724	0.727	0.727
Fuel temperature (K)					
Min	613.40	601.00	595.20	566.40	572.90
Max	1,268.30	1,276.00	1,288.10	1,358.40	1,227.50
Mean	963.89	982.74	956.65	884.69	891.59
Median	985.50	1,020.20	977.60	889.10	904.00
10%	656.41	657.49	667.14	628.60	639.50
25%	854.23	892.40	858.20	731.80	747.70
75%	1,103.48	1,108.80	1,087.30	1,019.60	1,036.60
90%	1,161.89	1,170.02	1,158.90	1,137.90	1,105.40

3.2.2 BWR Average Assembly Burnup and Specific Power

Operating characteristics for the BWR/4-6 fuel assembly class based on the 2013 CG-859 survey data—including mean value and range for the assembly average burnup and specific power—are provided in Table 41. These characteristics for site-specific Big Rock Point, Dresden-1, and LaCrosse fuel assemblies are provided in Table 42.

Table 41. Operating characteristics for the BWR/4-6 fuel assembly class.

GC-859 assembly type code	G4607G3B	G4608G4B	G4609A	G4610G14	G4610A
Array size	7 × 7	8 × 8	9 × 9	10 × 10	10 × 10
Burnup mean (MWd/MTU)	21,948	22,760	34,515	44,432	43,299
Burnup range (MWd/MTU)	7,695–3,0831	13,379–32,941	3,000–45,000	4,782–53,453	6,516–52,016
Specific power mean (MW/MTU)	15.57	16.69	21.77	26.33	26.06
Specific power range (MW/MTU)	9.86–19.53	11.94–22.23	6.38–29.41	14.13–35.14	15.53–35.20

Table 42. Operating characteristics of site-specific assembly types Big Rock Point (XBR09A), Dresden-1 (XDR06G5), and LaCrosse (XLC10A).

GC-859 assembly type code	XBR09A	XDR06G5	XLC10A
Array size	9 × 9	6 × 6	10 × 10
Burnup mean (MWd/MTU)	20,981	21095	15,017
Burnup range (MWd/MTU)	19,061–22,811	9,065–25,886	4,678–20,126
Specific power mean (MW/MTU)	15.16	9.07	14.79
Specific power range (MW/MTU)	14.20-16.22	6.75-15.01	8.50-21.93

3.3 STAINELESS-STEEL REPLACEMENT RODS

In the United States, limited substitutions of Zr alloy or solid stainless-steel filler rods for fuel rods are allowed per Generic Letter 90-02 and its Supplement 1 guidance [54], dependent on technical specifications or other operational limits. If more than 30 rods in the core or 10 rods in any assembly are replaced during a refueling, a special report that describes the number of rods replaced must be submitted according to the guidance. Information about the maximum number of filler rods in discharged fuel assemblies is not readily available. The 2013 GC-859 survey data reported that approximately 850 fuel assemblies contained replacement rods. However, these data provide specific information on the use of stainless-steel filler rods for less than 40 fuel assemblies. An SNF assembly discharged from the Maine Yankee reactor—the average burnup of which was 46.835 GWd/MTU over three irradiation cycles—contains four stainless-steel filler rods [55]. A reconstituted fuel assembly used in the R. E. Ginna nuclear plant had five stainless-steel replacement rods [56]. Technical and licensing information for North Anna Units 1 and 2 permits the use of up to 10 solid stainless-steel replacement rods per assembly [57].

4. AXIAL BURNUP PROFILES

Rod averaged burnup and peak pellet burnup values are currently limited to 62 and 70 GWd/MTU, respectively [58]. The BWR fuel has a higher ratio of peak pellet average burnup to peak assembly average burnup than the PWR fuel with the same batch average burnup. For example, the ratio values are ~1.5 and ~1.16 for the BWR and PWR fuel assemblies, respectively, with a batch average burnup of 45 GWd/MTU [59].

SNF assemblies exhibit radial and axial burnup variations. An axial burnup profile is typically considered in SNF applications. Typically, the most limiting dose rate for transportation packages is the radial dose rates at 2 m from the lateral surface of the transportation vehicle [60, 61]. Therefore, axial burnup profiles with high peaking factors are bounding with respect to the limiting radial dose rates of transportation packages because the SNF radiation source intensity increases with increasing burnup. The axial burnup profile peaking factor is defined as the ratio between the maximum and average values of the burnup profile. This section analyzes the PWR and BWR axial burnup profiles available from nonproprietary documents [11, 12] and identifies the PWR and BWR axial burnup profiles with high peaking factors for use in shielding analyses of SNF transportation packages.

4.1 PWR AXIAL BURNUP PROFILES

PWR axial burnup profiles are available for 3,175 PWR fuel assemblies with average burnup values from approximately 3.1 to 55.3 GWd/MTU [11]. The profiles are provided for 18 axial fuel zones of identical length. Bounding PWR axial burnup profiles for transportation package shielding analyses based on the analysis of the available axial burnup profiles are provided in Table 43. Bounding axial burnup profiles are provided for fuel assembly average burnup values less than 18 GWd/MTU, 18–30 GWd/MTU, 30–45 GWd/MTU, and greater than 45 GWd/MTU. The axial peaking factor for each axial burnup profile is highlighted in the table. The axial burnup profiles provided in Table 43 are from blanketed WE fuel assemblies. These profiles bound the axial burnup profiles of non-blanketed PWR fuel assemblies and are conservative with respect to external radial dose rates of SNF transportation packages.

Table 43. Bounding PWR axial burnup profiles for transportation package shielding analysis.

Axial zone no. [a]	Burnup <18 GWd/MTU	18 ≤ burnup < 30 GWd/MTU	30 ≤ burnup < 45 GWd/MTU	60 > burnup ≥ 45 GWd/MTU
1	0.216	0.279	0.274	0.328
2	0.772	0.899	0.882	0.932
3	0.959	1.097	1.044	1.102
4	1.024	1.168	1.095	1.159
5	1.076	1.182	1.128	1.169
6	1.155	1.178	1.154	1.164
7	1.202	1.169	1.162	1.157
8	1.221	1.160	1.169	1.149
9	1.219	1.152	1.168	1.142
10	1.208	1.145	1.160	1.135
11	1.198	1.139	1.151	1.133
12	1.198	1.133	1.147	1.112
13	1.183	1.125	1.139	1.108
14	1.163	1.109	1.123	1.095
15	1.129	1.072	1.094	1.064
16	1.028	0.978	1.012	0.983
17	0.811	0.774	0.830	0.800
18	0.237	0.240	0.268	0.269

[a] Bottom to top; zone #1 corresponds to the bottom of the active fuel.

4.2 BWR AXIAL BURNUP PROFILES

A total of 2,213 BWR axial burnup profiles are provided in the Framatome ANP 32-5045751-00 report titled *BWR Axial Burnup Profile Evaluation* [12]. These axial burnup profiles, representative of BWR blanketed and non-blanketed fuel assemblies [62], were developed by using CRC axial burnup data from Grand Gulf Unit 1 cycles 2–8 and end-of-cycle 13, LaSalle Unit 1 cycles 4–8, and Quad Cities Unit 2 cycles 9–14. Profiles are provided for assembly average burnup less than 6 GWd/MTU, for 6–46 GWd/MTU in 4 GWd/MTU increments, and for assembly average burnup greater than 46 GWd/MTU. The profiles are provided for 25 axial fuel zones of identical length. The BWR axial burnup profiles provided in the Framatome ANP report were analyzed, and the profiles with highest peaking factors were identified. The BWR fuel assemblies analyzed in the Framatome ANP 32-5045751-00 report do not contain part-length rods. Partial length fuel rods and inner channels are used in current BWR fuel assemblies to achieve a more homogeneous burnup distribution in the fuel [63]. Therefore, the axial burnup profiles of BWR fuel assemblies with partial length fuel rods are expected to be flatter than the axial burnup profiles of fuel assemblies with full length fuel rods.

Table 44 provides the maximum values for the axial peaking factors identified within 12 average fuel assembly burnup intervals. The bottom half of a BWR fuel assembly typically achieves higher burnup than the upper half. However, a more uniform burnup axial burnup profile is achieved with increasing assembly average burnup. Bounding BWR axial burnup profiles for transportation package shielding analysis are provided in Table 45.

Table 44. Maximum axial peaking factor as a function of burnup range for the evaluated BWR fuel assemblies.

Assembly average burnup (GWd/MTU)	Axial peaking factor
<6	1.567
6–10	1.418
10–14	1.527
14–18	1.515
18–22	1.335
22–26	1.366
26–30	1.415
30–34	1.372
34–38	1.302
38–42	1.301
42–46	1.287
>46	1.267

Table 45. Bounding BWR axial burnup profiles for transportation package shielding analysis.

	Burnup (GWd/MTU)											
Axial zone no. [a]	<6	6–10	10–14	14–18	18–22	22–26	26–30	30–34	34–38	38–42	42–46	>46
25	0.105	0.125	0.085	0.086	0.156	0.159	0.103	0.112	0.153	0.160	0.172	0.159
24	0.171	0.216	0.166	0.166	0.429	0.441	0.198	0.212	0.252	0.258	0.276	0.264
23	0.447	0.539	0.468	0.457	0.601	0.600	0.537	0.559	0.571	0.571	0.591	0.596
22	0.555	0.674	0.610	0.597	0.740	0.728	0.694	0.716	0.754	0.746	0.759	0.771
21	0.621	0.789	0.681	0.671	0.830	0.804	0.784	0.805	0.886	0.876	0.883	0.900
20	0.702	0.853	0.750	0.744	0.935	0.883	0.858	0.878	0.968	0.960	0.963	0.985
19	0.766	0.909	0.813	0.813	0.998	0.938	0.917	0.937	1.018	1.013	1.016	1.044
18	0.817	0.964	0.879	0.884	1.028	0.973	0.971	0.991	1.067	1.062	1.065	1.092
17	0.883	1.043	0.948	0.955	1.065	1.019	1.021	1.039	1.114	1.106	1.111	1.134
16	0.971	1.090	0.960	0.968	1.105	1.072	1.021	1.039	1.082	1.076	1.084	1.099
15	1.108	1.126	1.031	1.038	1.126	1.107	1.070	1.086	1.124	1.116	1.124	1.134
14	1.173	1.158	1.102	1.107	1.143	1.133	1.120	1.133	1.161	1.152	1.162	1.166
13	1.251	1.189	1.172	1.175	1.183	1.177	1.167	1.179	1.193	1.185	1.196	1.192
12	1.301	1.219	1.262	1.257	1.211	1.207	1.214	1.224	1.221	1.215	1.229	1.214
11	1.333	1.248	1.321	1.311	1.234	1.227	1.264	1.268	1.246	1.241	1.255	1.234
10	1.378	1.276	1.366	1.352	1.271	1.259	1.300	1.297	1.266	1.261	1.275	1.249
9	1.422	1.298	1.406	1.386	1.302	1.287	1.328	1.316	1.279	1.274	1.286	1.258
8	1.462	1.281	1.443	1.415	1.325	1.312	1.355	1.328	1.292	1.286	1.287	1.264
7	1.512	1.312	1.480	1.444	1.335	1.340	1.380	1.341	1.302	1.296	1.268	1.267
6	1.561	1.362	1.511	1.480	1.318	1.364	1.402	1.357	1.302	1.301	1.266	1.267
5	1.567	1.413	1.527	1.515	1.300	1.366	1.415	1.372	1.288	1.294	1.261	1.256
4	1.472	1.418	1.493	1.513	1.243	1.311	1.393	1.356	1.245	1.259	1.229	1.219
3	1.263	1.288	1.330	1.386	1.094	1.169	1.271	1.246	1.125	1.150	1.123	1.114
2	0.927	0.952	0.963	1.030	0.812	0.887	0.965	0.955	0.853	0.888	0.869	0.869
1	0.233	0.258	0.233	0.249	0.217	0.241	0.254	0.254	0.237	0.252	0.250	0.254

[a] Top to bottom; zone #1 corresponds to the bottom of the active fuel.

4.3 EFFECTS OF AXIAL BLANKET ON AXIAL POWER PEAKING

A previous axial blanket demonstration program [21] showed that the PWR blanketed fuel assembly had an increase in assembly axial power peaking of 12.2% at beginning of life and 6.8% at 325 EFPDs relative to non-blanketed fuel (i.e., the increase in axial power peaking decreases with increasing burnup and irradiation time). The most economical option found by this demonstration program for the U enrichment in the blanket regions was natural U. Typically, the top and bottom 6 in. of enriched U are replaced with natural U in blanketed fuel. Blanketed fuel is characterized by a more pointed axial burnup profile compared with non-blanketed fuel [16]. However, optimum axial power shaping in blanketed cores can be achieved with fuel axial enrichment zoning [64].

5. NFH PHYSICAL CHARACTERISTICS AND OPERATING CONDITIONS

Nuclear power reactors contain non-fuel components that are not an integral part of the fuel assembly. However, irradiated PWR non-fuel components are usually inserted into the guide tubes of the PWR SNF assemblies loaded in storage canisters. NFH physical characteristics and irradiation conditions are input parameters to activation source and radiation dose rate calculations. This section provides available data on physical characteristics and irradiation conditions of PWR control rods, burnable poison rod (BPR) assemblies (BPRAs), neutron source assemblies (NSAs), orifice rod assemblies (ORAs), and thimble plug devices (TPDs). The data were primarily obtained from the CRC [8], DOE/RW-0184 [1,3], and PNL-8425 [4] reports.

Vendors use different names to refer to their neutron absorbing components. Thus, control rod assembly (CRA), rod cluster control assembly (RCCA), and control element assembly (CEA) are used to indicate B&W, WE, and CE neutron absorbing components, respectively. B&W NFH includes CRAs, axial power-shaping rod assemblies (APSRAs), BPRAs, ORAs, and NSAs. WE NFH includes RCCAs, BPRAs, TPDs, and NSAs. CE NFH includes CEAs and NSAs. Similar information is provided for irradiated BWR control blades, which are considered Greater-Than-Class-C radioactive waste [65].

The NFH activation source varies as a function of its axial exposure location in the reactor during full-power operation and the NFH material weight and elemental composition corresponding to that axial exposure location. This section provides the data available in the DOE/RW-0184 report [3] for the materials and weights of NFH at various exposure locations during full-power operation. The exposure zones are subdivided into above UEF, UEF, GP, in core (i.e., active fuel), LEF, and below LEF regions [3]. The depth of insertion into these regions varies depending on the NFH type. For example, an RCCA might be fully withdrawn at all times during full-power operations. However, the exposure locations of the RCCA tip include the assembly GP and UEF regions at all times during full-power operations.

5.1 CONTROL RODS

Control rods are used to shape the axial power distribution of the core and provide reactivity control of the fuel core. CRAs, RCCAs, and CEAs contain control rods sized to fit within the assembly guide tubes. The individual control rods are attached by a metal bracket, called a “spider,” at the top. Neutron absorbing materials used in control rods include B_4C, Ag-In-Cd alloy, Hf metal, and stainless steel with B of which 80% is ^{10}B [4]. Various models with full-length and partial-length control rods exist. Hybrid full-length control rods contain Ag-In-Cd alloy and B_4C or Hf metal and B_4C. The PWR control rods are inserted from the top of the fuel assembly, whereas the BWR control rods are inserted from the bottom of the fuel assembly.

5.1.1 CRA, RCCA, and CEA Design Data

Available design data for a CRA (B&W 15 × 15 assembly) [4, 8] and a full length 24-rod RCCA (WE 17 × 17 assembly) [4, 7] are presented in Table 46.

Table 46. B&W CRA and WE RCCA design data.

Characteristic	CRA [8]	RCCA [7]
Number of control rods	16	24
Overall length (cm)	406.4 [4]	408.7 [4]
Pellet material	Ag-In-Cd	Ag-In-Cd
Fraction of pellet materials	Ag(79.8%), In(15.0%), Cd(5.0%)	Ag(80.0%), In(15.0%), Cd(5.0%)
Pellet density (g/cm^3)	10.17	10.16
Pellet OD (cm)	0.99568	0.86614
Clad material	SS304	SS304
Clad OD (cm)	1.11760	0.96774
Clad ID (cm)	1.01092	0.87376
Absorber region length (cm)	340.361	360.68
Lower end plug material	SS304	SS304
Lower end plug length (cm)	2.684	1.87
Plenum spring material	SS302	Inconel
Plenum spring length (cm)	27.813	12.001
Spider assembly material	SS CF3M, SS 304, and SS 316 [4]	SS 304, SS 308, and Inconel X-750 [4]

A typical CEA for the CE 14 × 14 and 16 × 16 standard lattices has four or five fingers attached to a spider. The 16 × 16 System 80 plants (C8016C assembly code) might use a 12, 8, or 4 element CEA. Partial- and full-length CEAs exist. Available design data for full-length CEA are presented in Table 47.

Table 47. CEA design data.

Characteristic	12-finger CEA [3]	San Onofre full length CEA [3]
Number of control rods	12	5 or 4
Total length (cm)	642.62 (253 in.)	459.74 (181 in.)
Total weight (kg)	87.18 (192.2 lb)	32.66 (72 lb)
Cladding material	Inconel 625	Inconel 625
OD (cm)	2.073 (0.816 in.)	2.073 (0.816 in.)
Wall thickness (cm)	0.0889 (0.035 in.)	0.0889 (0.035 in.)
Primary poison material	B_4C	B_4C [b]
Poison length (cm)	375.92 [a] (148 in.)	377.19 (148.5 in.)
Pellet diameter (cm)	1.872 (0.737 in.)	1.872 (0.737 in.)
Plenum spring material	SS302	SS302
Spider material	SS304	SS304

[a] 31.75 cm (12.5 in.) long segment of felt metal and reduced diameter B_4C pellets and 344.17 cm (135.5 in.) long segment of B_4C pellets [4]. The length of the rod tip is 3.81 cm (1.5 in.).
[b] A CEA might contain both B_4C and Ag-In-Cd alloy [4].

Material weights at differed exposure locations were evaluated in the DOE/RW-0184 report [3] and are provided in Table 48.

Table 48. Weights of NFH at various exposure locations.

Material	Total weight (kg)	Exposure zone
B&W standard CRA		
SS CF3M	3.2	Top
SS 304	0.07	Top
Ag-In-Cd	43.12	In core
SS 304	10.82	In core
SS 302	0.85	In core
WE full length RCCA		
SS 302	0.50	Top
SS 308M	1.10	Top
Inconel-718	0.75	Top
SS 304	13.0	GP
Ag-In-Cd	51.8	GP
12-finger CEA		
SS 304	8.17	Top
Inconel 625	53.62	Top
B_4C	20.90	Top
SS 304	0.68	GP
Inconel 625	2.2	GP
B_4C	1.6	GP
San Onofre full length CEA		
SS 304	3.40	Top
Inconel 625	15.50	Top
B_4C	8.71	Top
Ag-In-Cd	1.10	Top
SS 304	0.23	GP
Inconel 625	0.91	GP
Ag-In-Cd	2.80	GP

5.1.2 CRA/RCCA/CEA Insertion Data

Information on the percentage of the CRA/RCCA/CEA at a certain axial exposure location and estimated exposure lifetime from the DOE/RW-0184 report [1] are provided in Table 49.

Table 49. Estimated exposure locations and lifetime of CRA/ RCCA/CEA.

	Exposure location				
	Above top end fitting	Top end fitting	GP	In core	
Type	**Percentage of the component at locations (%)**				**Exposure lifetime [a] (in cycles)**
CRA	83	5	5	7	10
RCCA	90	5	5	–	10
CEA	70	15	15	–	10

[a] Three cycles per assembly lifetime.

Specific CRA and RCCA insertion data are available from the YMP summary reports for the Crystal River Unit 3 cycles 1–10 [8], and McGuire Unit 1 cycles 1–7 [7] power reactors, respectively. Crystal River Unit 3 data are available for two CRA groups used in cycles 1–10. One group was withdrawn between 83 and 100% (e.g., completely withdrawn during cycles 5–10) during full-power operations. The other group was mostly inserted during cycles 1–4 (e.g., from 79 to 96.5%, except for at the end of cycles 3 and 4 when it was ~85% withdrawn), and then it was mostly withdrawn (~80–100%), starting with the end of cycle 4. The reported insertion data for the WE RCCA indicate that an RCCA was either fully withdrawn or inserted in either the top 22.86 cm of the active fuel region of a fuel assembly for approximately 62–125 EFPDs or in the top 45.72 cm of the active fuel region of a fuel assembly for approximately 17–33 EFPDs.

The irradiation history of a spent RCCA, discharged after 12 cycles and 102,767 h of service from the WE PWR Point Beach 1 power reactor, is provided in the PNL-10103 report [65]. Table 50 provides the cycle burnup values of the host assemblies. The RCCA comprised 16 Ag-In-Cd rods designed to fit a 14 × 14 fuel lattice. The RCCA was fully withdrawn at all times during full-power operations. The tip, which was nearest the core, was highly activated. Elemental analyses were performed for samples taken from activated metal. Activation dropped off to negligible levels beyond a short distance less than 2 ft from the core. The assumed applicable flux scaling factor for the component region within 12 in. of core periphery (i.e., CRA end caps) was 0.1.

Table 50. RCCA irradiation history.

Cycle	Host assembly burnup (MWd/MTU)
1	18,770
2	10,721
3	13,932
4	8,225
5	10,141
6	8,830
7	9,351
8	8,417
9	7,313
10	8,180
11	7,916
12	13,793
Total	125,589

5.1.3 B&W APSRA

APSRAs are only used in the B&W power reactors [8]. There are two types of APSRAs: a black APSRA that uses Ag-In-Cd as neutron absorber and a gray APSRA that uses Inconel as neutron absorber. Available design data for black and gray ASPRAs are provided in Table 51.

Table 51. B&W black and gray APSRAs.

Characteristic	Black APSRA [8]	Gray APSRA [8]
Number of rods	16	16
Overall length (cm)	406.4 [4]	405.765 [4]
Pellet material	Ag-In-Cd	Inconel 600 [4]
Fraction of pellet materials	Ag(79.8%), In(15.0%), Cd(5.0%)	–
Pellet density (g/cm^3)	10.17	8.3
Pellet OD (cm)	0.99568	0.95250
Clad material	SS304	SS304
Clad OD (cm)	1.11760	1.11760
Clad ID (cm)	1.01092	0.98044
Absorber region length (cm)	91.44	160.02
Lower end plug material	SS304	SS304
Lower end plug length (cm)	1.924	1.924
Length of the water inside clad	243.014	204.788
Spider assembly material	SS CF3M, SS 304, and SS 316	SS CF3M, SS 304, and SS 316

Starting from bottom to top, a black ASPRA rod comprises a lower SS304 plug (1.924 cm), a spacer (0.762 cm), the absorber (91.44 cm), a gap (4.953 cm), an intermediate plug (1.27 cm), water inside the clad (243.014 cm), and an upper end plug (0.635 cm). When fully inserted, the distance between the tip of the black ASPRA lower end plug and the bottom of the active fuel is 16.809 cm.

Starting from bottom to top, a gray ASPRA rod comprises a lower SS304 plug (1.924 cm), the absorber (160.02 cm), a gap (0.952 cm), an intermediate plug (1.905 cm), water inside the clad (204.788 cm), and an upper end plug (0.635 cm). When fully inserted, the distance between the tip of the gray ASPRA lower end plug and the bottom of the active fuel is 17.444 cm.

Table 52 provides the material weights at different exposure locations evaluated in the DOE/RW-0184 report [3].

Table 52. APSRA materials at various exposure locations.

Material	Total weight (kg)	Exposure zone
Black APSRA		
SS CF3M	3.5	Top
SS 304	0.073	Top
Ag-In-Cd	10.61	In core
SS 304	11.10	In core
Gray APSRA		
SS CF3M	3.4	Top
SS 304	0.07	Top
SS 304	13.5	In core
Inconel 600	15.3	In core

Table 53 provides information on the percentage of the APSRA at a certain axial exposure location and the estimated exposure lifetime from the DOE/RW-0184 report [1].

Table 53. Estimated exposure locations and lifetime of APSRA.

Exposure location			
UEF	GP	In core	
Percentage of the component at location (%)			**Exposure lifetime [a] (in cycles)**
14	5	81	5

[a] Three cycles per assembly lifetime.

Specific APSRA insertion data are available from the YMP summary report for the Crystal River Unit 3 cycles 1–10 [8]. Data are available for a black APSRA used during cycles 1–5 and a gray APSRA used during cycles 6–10. On average, the black APSRA was inserted approximately 90% during the first cycle of operation and approximately 75% thereafter. The gray APSRA was inserted approximately 70% during cycles 6–10. The active fuel region approximately 200–300 cm from its top was exposed to the black APSRA neutron absorber. The active fuel region approximately 75–240 cm from its top was exposed to the gray APSRA neutron absorber.

5.1.4 BWR Control Blade Design

Control rods are used to shape the axial power distribution in the lower portion of the core—yielding a more optimum fuel burnup—and to provide reactivity control of the fuel core. There are numerous control blade designs. The original control blade designs were replaced with new designs that are low in Co to reduce activation products, use Hf in the high-duty blade areas to reduce absorber swelling, and contain higher boron loadings effectively reducing the ^{10}B depletion rate [66]. A typical control rod consists of four blades placed into a cruciform shape. Each blade consists of welded absorber tubes filled with vibratory compacted B_4C powder. Some control rods might also contain unclad solid rods of Hf metal at the top and edges of control blades, which are high-flux areas, to extend control blade lifetime [16, 67]. All-Hf absorber control blades also exist for use in BWR control cell locations [66]. Table 54 provides the BWR control blade data.

Table 54. BWR control blade data.

Blade Data	Peach Bottom [a]	GE Reference design [b, c]	Marathon design [d]
Absorber material	B_4C	B_4C	B_4C
Density (g/cm^3)	–	1.76	–
B_4C absorber density (% theoretical density)	70%	70%	Minimum of 76.5%
^{10}B enrichment by weight	–	–	Minimum of 18%
Control length (cm)	363.22	363.22–365.76	–
Absorber tube material	SS304	SS304	Stainless steel
Blade span total (cm)	24.765	24.765–24.9174	–
Blade span central support (cm)	3.97002	–	–
Blade thickness total (cm)	0.79248	–	–
Blade thickness of sheath (cm)	0.14224	0.0762	–
Absorber tube ID (cm)	0.35052	0.35052	0.4508
Absorber tube OD (cm)	0.47752	0.47752	0.5588
Total number of absorber tubes	84	76[f]	68
Handle length (cm)	–	15.24	–
Base length (cm)	–	60.96	–
Total length (cm)	–	441.325	–
Sheath material [e]	–	SS304	–
Total weight (kg)	–	98.883–102.058	–
Structural material [d]	–	Stainless steel	–

[a] [68], [b] [4], [c] [67], [d] [16], [e] [65].
[e] The absorber tube and sheath in the Marathon design was replaced with an array of square outer envelope tubes [66]. This design consists of several configurations of B and/or mixed B and Hf poisons.
[f] The stiffener replaces two absorber rods [67].

5.1.5 BWR Control Blade Exposure Limits

Table 55 provides available data on estimated axial exposure locations and lifetime BWR control blades [1].

Table 55. Estimated exposure locations and lifetime of BWR cruciform control blades.

Exposure location			
In core	LEF	Below LEF	
Percentage of the component at locations (%)			Exposure lifetime [a] (in cycles)
15	5	80	10

[a] Four cycles per assembly lifetime.

A control blade is discharged from the reactor based on ^{10}B depletion or structural integrity issues. The calculation method for determining the percent ^{10}B depletion is based on correlations between smeared thermal fluence (in units of snvt) and ^{10}B depletion, where 1 snvt = 10^{21} n/cm^2. Exposure limits depend on blade design. The original GE equipment has a mechanical lifetime equivalent to 34% ^{10}B depletion due to absorber tube cracking and crevice corrosion. However, these blades were replaced with a design that incorporates better materials, Hf, and higher B_4C loadings, which extended blade lifetime to about three times that of the original equipment blade. GE marathon design has an exposure limit of ~5.0 snvt. Exposure limits for the original equipment of Siemens design varies from 1.6 to 2.7 snvt. A fluence of

~10^{22} n/cm^2 was used at a utility as the criterion for avoiding material embrittlement [66]. Some utilities practice bladed shuffling by moving blades from high-duty positions to lower duty positions, which increases blade lifetime, whereas other utilities do not shuffle blades for economic reasons.

The irradiation history of a GE control blade discharged from the Duane Arnold power reactor is provided in the PNL-10103 report [65]. This blade was used during 10 operation cycles at two reactor core locations. It was completely withdrawn during cycles 5, 7, 8, and 9. The blade was inserted to various levels in the core during its exposure. The insertion data presented in Table 56 were extracted from the graphs available in the PNL-10103 report and might be imprecise. The neutron exposure during full insertion is extremely low because the reactor was either coasting down or at the zero-power level [65].

Table 56. Control blade insertion data by cycle

Cycle	Cycle EFP hours	Percent inserted (%)	EFP hours	Percent inserted (%)	EFP hours	Percent inserted (%)	EFP hours	Percent inserted (%)	EFP hours
1	5,150	70	600	80	800	90	300	100	200
2	5,500	50	100	60	200	70	100	80	550
3	4,650	40	550	50	1,000	60	250	100	200
4	3,650	70	650	80	300	90	700	100	200
5	2,830	–	–	–	–	–	–	–	–
6	4,800	70	1,300	100	200				
7	3,450	–	–	–	–	–	–	–	–
8	4,250	–	–	–	–	–	–	–	–
9	3,250	60	700	70	600	80	150	100	50
10	9,200	–	–	–	–	–	–	–	–

At discharge, the ^{10}B depletion values in each of the four quarters of the control rod length were 7.89, 21.16, 31.69, and 30.73% (from bottom to top). This depletion in terms of snvts units was 0.48, 1.46, 1.91, and 1.85 snvts. ^{60}Co measurements on samples taken at various axial locations along the blade were ~ 2,000 μg/g for the handle and tip and an approximately uniform 1,200 μg/g for the sheath.

5.2 BPRA

BPRAs are inserted into the guide tubes of a PWR fuel assembly during operation. These absorber rods are not an integral part of the fuel assembly and are typically removed after one irradiation cycle. There are several different general types of BPRAs. The B&W BPRAs comprise $Al_2O_3 – B_4C$ pellets in Zircaloy tubing. The documented B_4C loading in the B&W BPRAs varies from 0 to 2.1%. WE BPRAs comprise either Pyrex glass ($B_2O_3 – SiO_2$) with 12.5 wt % B_2O_3 sealed in stainless-steel cladding or hollow Pyrex glass ($B_4C – Al_2O_3$ with 14.0 wt % B_4C) sealed in Zircaloy cladding. The former is referred to as *burnable absorber assembly (BAA)*, and the latter is referred to as *wet annular burnable absorber (WABA)*. BPRAs are not used in CE power reactors.

5.2.1 B&W BPRA Design Data

Table 57 provides the design data available for the Crystal River Unit 3 BPRA [8].

Table 57. B&W BPRA design data.

Characteristic	Value
Number of BPRs per assembly	16
Pellet material	$Al_2O_3 – B_4C$
Pellet density (g/cm^3)	3.7
Pellet OD (cm)	0.8636
Cladding material	Zircaloy
Clad OD (cm)	1.0922
Clad ID (cm)	0.9144
Absorber region length (cm)	320.04
Lower end plug material	Zircaloy
Lower end plug length (cm)	1.914
Distance between top of active fuel and top of burnable poison	17.78
Spider assembly material	Steel
Spider assembly length above active fuel region (cm)	32.045

5.2.2 WE BPRA Design Data

Table 58 provides the available WE BPRA design data [10, 4]. The WE BPRA dimensions and enrichments are provided for the WE 17 × 17 assembly class. Slightly different dimensions for the WE BPRAs are provided in the *Westinghouse Technology Systems Manual* [19].

Table 58. WE BPRA design data.

WE 17 × 17 assembly class		
Characteristic	**BAA**	**WABA**
Burnable poison material	B_2O_3-SiO_2	Al_2O_3-B_4C
Boron loading	12.5 wt % B_2O_3	14.0 wt % B_4C
^{10}B content	0.00624 g ^{10}B/cm	0.006165 g ^{10}B/cm
Burnable poison density (g/cm^3)	2.29900	2.59300
Burnable poison OD (cm)	0.85344	0.80770
Burnable poison ID (cm)	0.48260	0.70610
BPR clad material	SS 304	Zircaloy-4
BPR outer clad OD (cm)	0.96774	0.96774
BPR outer clad ID (cm)	0.87376	0.83570
BPR inner clad OD (cm)	0.46101	0.67820
BPR inner clad ID (cm)	0.42799	0.57150
Absorber length (cm)	360.68	340.46
Lower cap region (cm)	1.898	1.778
Upper plenum length (cm)	20.294	31.724
Number of BPRs per assembly	4–24	4–24
Overall length (cm)	396.494–398.018	390.144
Rod length (cm)	387.096	381
Assembly weight (kg)	6.85–22.82	6.90–23.45

5.2.3 BPRA Irradiation History Data

BPRAs are typically removed after one irradiation cycle. The burnup reported in the PNL-10103 report [65] for a spent BPRA discharged from the WE PWR Point Beach 1 power reactor is ~16,500 MWd/MTU. However, the burnup of a fuel assembly in modern PWR cores is much higher (e.g., 28.8 GWd/MTU in a 24-month cycle [69]). Table 59 provides information on the percentage of the BPRA at a certain axial exposure location and estimated exposure lifetime from the DOE/RW-0184 report [1].

Table 59. Estimated exposure locations of BPRA.

	Exposure location			
	UEF	GP	In core	
Type	**Percentage of the component at locations (%)**			**Exposure lifetime [a] (in cycles)**
B&W BPRA	14	5	81	1
WE BPRA	15	7	78	1

[a] Three cycles per assembly lifetime.

5.3 ORA and TPD

ORAs and TPDs are inserted into empty burnable poison locations in B&W and WE power reactors, effectively blocking the flow of coolant through empty guide tubes. Table 60 provides information on the percentage of standard ORA and TPD and the material composition at the top end fitting and GP exposure locations from the DOE/RW-0184 report [1]. The estimated ORA/TPD exposure lifetime is 20 years.

Table 60. Estimated exposure locations, lifetime, and material composition of ORA and TPD.

	Exposure location			
	UEF		GP	
Type	**Percentage of the component at location (%)**			
ORA	50		50	
TPD	50		50	
Type	**Material at location**	**Weight (kg) at location**	**Material at location**	**Weight (kg) at location**
ORA	SS CF3M	3.5	SS 304	3.4
	SS 304	0.07	–	–
TPD for WE 14 × 14	SS 304	1.7	SS 304	2.2
	Inconel-718	0.42	–	–
TPD for WE 15 × 15	SS 304	1.8	SS 304	2.7
	Inconel-718	0.42	–	–
TPD for WE 17 × 17	SS 304	2.3	SS 304	3.2
	Inconel-718	0.42	–	–

5.4 NEUTRON SOURCE ASSEMBLIES

Primary neutron sources, typically Cf capsules, are used for the initial startup and secondary neutron sources constructed of Sb-Be are employed in subsequent startups. Both neutron source assemblies consist of a burnable poison assembly with several poison rods replaced by source rods. Material weight and exposure data for a WE secondary NSA with 20 BPRs for the 17 x 17 fuel assembly are summarized in Table 61 [3] and Table 62 [1], respectively.

Table 61. NSA design data.

Design data			
Number of source rods		4	
Number of absorber rods		20	
Secondary source material		Sb-Be	
Source length (cm)		223.52	
Component location			
Top		In core	
Material at location	**Weight (kg)**	**Material at location**	**Weight (kg)**
SS 304	2.3	SS304	11.9
Inconel-718	0.42	Borosilicate glass	6.4
		Sb-Be	1.9

Table 62. Estimated NSA exposure locations and lifetime.

	Exposure location			
	UEF	GP	In core	
Type	**Percentage of the component at locations (%)**			**Exposure lifetime [a] (in cycles)**
B&W	17	4	79	7
WE	14	6	80	7
CE	10	2	88	10

[a] Three cycles per assembly lifetime.

6. DATA RELATED TO COBALT ACTIVATION SOURCE IN FUEL AND NON-FUEL HARDWARE MATERIALS

6.1 COBALT IMPURITY CONCENTRATION IN STAINLESS STEEL AND INCONEL ALLOYS

Fuel assembly hardware and NFH components typically contain stainless steel and Inconel alloys. Neutron activation of the Co impurity in these alloys produces the ^{60}Co radioisotope, which is a main source of gamma radiation [70, 71] with a half-life of 5.271 years. The quantity of the Co impurity is the most important parameter in determining whether the hardware contribution is significant [26]. Cobalt-60 is produced almost entirely by thermal and epithermal caption reactions in ^{59}Co [72]. Other production modes, such as ^{60}Ni(n,p)^{60}Co, ^{63}Cu(n,α)^{60}Co, and ^{58}Fe(n,γ)^{59}Fe $\xrightarrow{\beta^-}$ ^{59}Co, are insignificant based on low cross-section values and/or low parent nuclide concentrations [72,73]. Improved WE fuel assembly designs that use low Co stainless steel have been produced [19]; however, the permissible concentration levels of the Co impurity in hardware materials were not found in open literature.

Properties of alloys are specified by various material standards, such as American Society of Mechanical Engineers standards. However, concentration limits of trace elements are not specified in these standards, and the manufacturer is not required to report them. A recent report by Häkkinen [38] reviewed publicly available information on the Co concentration in fuel assembly materials. This section provides the Co impurity concentration levels in non-fuel materials from power reactors (see Table 63), which were documented in the DOE/RW-0184-R1 [1] and in Häkkinen [38] . The Co impurity concentration in Inconel-718 might be high (0.5–1%) because this alloy is primarily produced for aerospace applications [74]. However, the Co impurity is specified as 0.05% maximum for high Ni alloys for nuclear applications [75] because high concentrations of this impurity in contact with the coolant are undesirable.

Table 63. The range of Co impurity concentration in common reactor materials.

Material	Co concentration [a] (ppm)	Co concentration [b] (ppm)
Zircaloy-2	10	2-20
Zircaloy-4	10	2-20
Inconel-718	4,694	4,694–10,000
Inconel X-750	6,485	300–10,000
Stainless Steel 304	800	800
Stainless Steel 302	800	N/A
Nicrobraze 50	381	N/A

[a] [1]. [b] [38].

6.2 ORIGEN SCALING FACTORS FOR SNF HARDWARE REGIONS

Calculating Co activation sources in SNF assembly hardware materials requires determining average neutron flux and spectrum in the hardware regions that are outside the fueled region of the reactor. A simplified estimation method that applies bounding flux scaling factors to the activation products calculated with ORIGEN is commonly used to determine radiation source terms for fuel assembly hardware regions. The neutron flux and spectrum in the fueled region of the reactor are specified in ORIGEN activation calculations. The PNL-6906 Vol. 1 report [13] provides ORIGEN flux scaling factors that were empirically derived from laboratory analyses of 38 samples of activated hardware from three different SNF assemblies. These scaling factors and associated uncertainty are presented in Table 64.

Table 64. ORIGEN flux scaling factors from PNL-6906 Vol. 1.

Region	WE and B&W assemblies [a]	CE assemblies [a]	GE assemblies [a]
Top end fitting	0.1	0.05	0.1
GP	0.2	0.2	0.2
Fueled region	1.0	1.0	1.0
LEF	0.2	0.2	0.15

[a]The values have an uncertainty of ±50% [13].

ORIGEN scaling factors were evaluated in this report using a Monte Carlo N-Particle [76] detailed geometry model of a PWR core, which was developed based on Virtual Environment for Reactor Applications benchmark specifications [77]. The fuel assembly type in this core model is WE 17 × 17.

This calculation used the following.

- A neutron fission source with Watt energy spectrum and uniform spatial distributions. Therefore, the fission source spatial distribution is conservative with respect to the neutron flux in the fuel hardware regions because the axial neutron leakage is neglected in this model.
- A tally mesh that enabled the calculation of average fluxes within each fuel assembly axial region.
- The F4 (track length estimate of the average fluence) tally modified by the radiative (microscopic) capture cross section.

The maximum flux scaling factors for the LEF, GP, and UEF calculated as the ratio of the ^{60}Co amount in each fuel assembly hardware region to the ^{60}Co amount in the fuel region were approximately 0.22, 0.22, and 0.05, respectively. These flux scaling factors are approximately the same as the ORIGEN flux scaling factors provided in the PNL-6906 Vol. 1 report [13]. This evaluation limited to a WE 17 × 17 core shows that the PNL-6906 ORIGEN flux scaling factors are adequate for conservative activation source estimations.

7. CONCLUSIONS AND RECOMMENDATIONS

Shielding analyses of SNF transportation packages and storage casks include SNF radiation source term, NFH activation source, and dose rate calculations. Many input parameters—including geometry data, material specifications, and bounding irradiation conditions for fuel assemblies and NFH—are used in these calculations. Publicly available information related to PWR and BWR nuclear fuel physical characteristics and operating conditions is consolidated in this report. The intent of this report is to provide reference information for use in shielding analyses of SNF transportation packages and storage casks. Most data are dated 1992 or older.

Physical characteristics are provided for main assembly classes B&W 15 × 15, CE 14 × 14 and 16 × 16; WE 14 × 14, 15 × 15, and 17 × 17; GE BWR/4-6 7 × 7, 8 × 8, 9 × 9, and 10 × 10; and site-specific fuel assemblies for the Haddam Neck, Indian Point Unit 1, Palisades, San Onofre Unit 1, Yankee Rowe, Big Rock Point, and Dresden Unit 1 power reactors. Representative operating conditions are provided for PWR and BWR fuel assemblies. These data include cycle-averaged moderator density, fuel temperature, and specific power, and B letdown curve data for the PWR fuel assemblies; and cycle-averaged moderator density, fuel temperature, and specific power for the BWR fuel assemblies. The range of initial enrichment and average assembly burnup are based on the 2013 CG-859 survey data.

Axial burnup profiles for PWR and BWR fuel assemblies that maximize the radial dose rates in the external regions of transportation packages and storage casks were identified among available axial burnup profiles. Physical characteristics and operating conditions are provided for PWR NFH, including control rods, burnable absorber assemblies, NSAs, ORAs, and TPDs, as well as for the BWR control rods.

Data related to Co activation source in fuel and NFH materials, including Co impurity concentrations in various steel and Inconel alloys and ORIGEN flux scaling factors, are also provided.

ACKNOWLEDGMENTS

The work described in this report was accomplished with funding provided by the US Nuclear Regulatory Commission.

8. REFERENCES

1. *Characteristics of Potential Repository Wastes*, DOE/RW-0184-R1, Volume 1, US DOE Office of Civilian Radioactive Waste Management, Washington, D.C. (1992).
2. Characteristics of Spent Fuel, High Level Waste, and Other Radioactive Wastes Which May Require Long-Term Isolation, DOE/RW-0184, Appendix 2A, Physical Descriptions of LWR Fuel Assemblies (1987).
3. *Characteristics of Spent Fuel, High-Level Waste, and other Radioactive Wastes which May Require Long-Term Isolation*, Appendix 2E: Physical Descriptions of LWR Nonfuel Assembly Hardware, DOE/RW-0184, Volume 5 of 6, US DOE Office of Civilian Radioactive Waste Management, Washington, DC (1987).
4. E. C. Hawkes, Physical Characteristics of Non-Fuel Assembly Reactor Components, PNL-8425 (1994).
5. R. S. Moore and K. J. Notz, Physical Characteristics of the GE BWR Fuel Assemblies, ORNL/TM-10902, Oak Ridge National Laboratory (1989).
6. Physical and Decay Characteristics of Commercial LWR Spent Fuel, ORNL/TM-9591, 1986.
7. *Summary Report of Commercial Reactor Criticality Data for McGuire Unit 1*, B00000000-01717-5705-00063 Rev. 01, Civilian Radioactive Waste Management System Management & Operating Contractor, prepared for US Department of Energy Yucca Mountain Site Characterization Project Office, Las Vegas, NV (1998).
8. *Summary Report of Commercial Reactor Criticality Data for Crystal River Unit 3*, B00000000-01717-5705-00060 Rev. 01, Civilian Radioactive Waste Management System Management & Operating Contractor, prepared for US Department of Energy Yucca Mountain Site Characterization Project Office, Las Vegas, NV (1998).
9. *Summary Report of Commercial Reactor Criticality Data for LaSalle Unit 1*, B00000000-01717-5705-00138 Rev. 00, Civilian Radioactive Waste Management System Management & Operating Contractor, prepared for US Department of Energy Yucca Mountain Site Characterization Project Office, Las Vegas, NV (1999).
10. *Summary Report of Commercial Reactor Criticality Data for Sequoyah Unit 2*, B00000000-01717-5705-00064 Rev. 01, Civilian Radioactive Waste Management System Management & Operating Contractor, prepared for US Department of Energy Yucca Mountain Site Characterization Project Office, Las Vegas, NV (1998).
11. R. J. Cacciapouti and S. Van Volkinburg, "Axial Burnup Profile Database for Pressurized Water Reactors," YAEC-1937, Yankee Atomic Electric Company (May 1997).
12. L. B. Wimmer and C. W. Mays, BWR Axial Burnup Profile Evaluation, 32-5045751-00, Framatome ANP, Lynchburg, VA (2004).
13. A. Luksic, "Spent Fuel Assembly Hardware: Characterization and 10CFR 61 Classification for Waste Disposal," Volume1-Activation Measurements and Comparison with Calculations for Spent Fuel Assembly Hardware, PNL-6906-vol. 1, Pacific Northwest Laboratory, June 1989.
14. "Nuclear Fuel Data Survey Form GC-859," Energy Information Administration, US Department of Energy, [Online]. Available: http://www.eia.gov/survey/form/gc_859/proposed/form.pdf. [Accessed 9/30/2020].

15. J. Hu et al., US Commercial Spent Nuclear Fuel Assembly Characteristics: 1968-2013, NUREG/CR-7227 (ORNL/TM-2015/619), US Nuclear Regulatory Commission (2015).

16. *General Electric Systems Technology Manual*, Chapter 2.2, Fuel and Control Rods System, Nuclear Regulatory Commission, ADAMS ML11258A302.

17. *LaSalle, Units 1 &2, Updated Final Safety Analysis Report*, LSCS-UFSAR (2014), Nuclear Regulatory Commission, ADAMS ML14113A088.

18. J. C. Wagner, et al., Categorization of Used Nuclear Fuel Inventory in Support of a Comprehensive National Nuclear Fuel Cycle Strategy, ORNL/TM-2012/308, Oak Ridge National Laboratory (2012).

19. *Westinghouse Technology Systems Manual*, Nuclear Regulatory Commission, ADAMS ML02304131.

20. *Incorporation of Chromia-Doped Fuel Properties in AREVA Approved Methods*, ANP-10340NP, Revision 0, AREVA (2016).

21. M. A. Hannah, Axial Fuel Blanket Design and Demonstration, First Semi-Annual Progress Report: January-September 1980, DOE/ET/34020-1, Babcock & Wilcox, Lynchburg, VA, (1980).

22. *Surry Power Station Proposed Technical Specification Changes*, NRC ADAMS ML18153B162.pdf.

23. J. S. Armijo, L. F. Coffin, and H. S. Rosenbaum, "Development of Zirconium—Barrier Fuel Cladding," in *Zirconium Production and Technology: The Kroll Medal Papers 1975–2010*, ed. R. Adamson (West Conshohocken, PA: ASTM International, 2010), 197-212.

24. R. A. LEFEBVRE et al., "Development of Streamlined Nuclear Safety Analysis Tool for Spent Nuclear Fuel Applications," *Nucl. Technol.*, 199, *3*, 227 (2017).

25. G. M. O'Donnell, H. H. Scott, and R. O. Meyer, A New Comparative Analysis of LWR Fuel Designs, NUREG-1754, US Nuclear Regulatory Commission (2001).

26. B. L. Broadhead, Recommendations for Shielding Evaluations for Transport and Storage Packages, NUREG/CR-6802, Nuclear Regulatory Commission (2003).

27. M. T. Pigni, S. Croft, and I. C. Gauld, Uncertainty Quantification in (α,n) Neutron Source Calculations for an Oxide Matrix, Progress in Nuclear Energy, Vol. 91, August 2016, Pages 147-152 (2016).

28. T. Murata and K. Shibata, Evaluation of the (α,n) Reaction Nuclear Data for Light Nuclei, Journal of Nuclear Science and Technology, Supplement 2, p. 76-79 (August 2002).

29. A. C. Fernandes at al., Comparison of thick-target (alpha,n) yield calculation codes, Proceedings, 13th International Conference on Radiation Shielding (ICRS-13) & 19th Topical Meeting of the Radiation Protection & Shielding Division of the American Nuclear Society - 2016 (RPSD-2016), Paris, France, October 3-6, 2016.

30. *Standard Specification for Uranium Hexafluoride Enriched to Less Than 5 % ^{235}U*, ASTM-C996-20, ASTM International (2020).

31. *Standard Specification for Uranium Hexafluoride for Enrichment*, ASTM-C787-20, ASTM International (2020).

32. *Standard Specification for Nuclear-Grade, Sinterable Uranium Dioxide Powder*, ASTM-C753, ASTM International (2016).

33. *Standard Specification for Nuclear-Grade, Nuclear-Grade Gadolinium Oxide (Gd_2O_3) Powder*, ASTM-C888-18, ASTM International (2018).

34. *Standard Specification for Sintered Uranium Dioxide Pellets for Light Water Reactors,* ASTM-C776-17, ASTM International (2017).

35. *Standard Specification for Nuclear-Grade, Sintered Gadolinium Oxide - Uranium Dioxide Pellets,* ASTM-C922-14, ASTM International (2014).

36. *Standard Practice for Determining Equivalent Boron Contents of Nuclear Materials,* ASTM-1233-15, ASTM International (2015).

37. T. L Spano et al., "Comparative chemical and structural analyses of two uranium dioxide fuel pellets," *Journal of Nuclear Materials*, 518 (2019) 149-161.

38. S. Häkkinen, Impurities in LWR fuel and structural materials, VTT-R-00184-20, VTT Technical Research Center of Finland, Ltd. (2019).

39. A. G. Croff et al., Revised Uranium-Plutonium Cycle PWR and BWR Models for the ORIGEN Computer Code, ORNL/TM-6051, Oak Ridge National Laboratory (1978).

40. B. T. Rearden and M. A. Jessee, Eds. 2016. *SCALE Code System*, ORNL/TM-2005/39, Version 6.2.1, Oak Ridge National Laboratory. Available from the Radiation Safety Information Computational Center as CCC-834.

41. *Optimum Discharge Burnup for Nuclear Fuel – A Comprehensive Study of Duke Power's Reactors*, TR-112571, Electric Power Research Institute (1999).

42. *Optimum Cycle Length and Discharge Burnup for Nuclear Fuel – A Comprehensive Study for BWRs and PWRs – Phase I: Results Achievable Within the 5% Enrichment Limit*, 1003133, Electric Power Research Institute (2001).

43. *The Economic Benefit and Challenges with Utilizing Increased Enrichment and Fuel Burnup for Light-Water Reactors*, Nuclear Energy Institute (2019).

44. Review of Accident Tolerant Fuel Concepts with Implications to Severe Accident Progression and Radiological Releases, ERI/NRC 20-209, Energy Research Inc. and US Nuclear Regulatory Commission (2020).

45. D. Ohai, Large Grain Size UO_2 Sintered Pellets Obtained for Burn up Extension, Transactions of the 17th International Conference on Structural Mechanics in Reactor Technologies (SMiRT 17), Prague, Czech Republic, August 17-22 (2003).

46. J. Arborelius et al., Advanced Doped UO_2 Pellets in LWR Applications, *Journal of Nucl. Sci. and Technol.*, Vol. 43, No. 9, p. 967-976 (2006).

47. M. H. A. Piro et al., Pellet-Clad Interaction Behavior in Zirconium Alloy Fuel Cladding, in Comprehensive Nuclear Materials (Second Edition), Elsevier (2020).

48. R. Hall et al., Extended-Enrichment Accident-Tolerant LWR Fuel Isotopic and Lattice Parameter Trends, ORNL/TM-2021/1961, Oak Ridge National Laboratory (2021).

49. H. Ohta, T. Sawabe, and T. Ogata, Accident-tolerant control rod, International Workshop on Accident Tolerant Fuels of LWRs, 10-12 Dec. 2012, NEA/NSC/DOC(2013)9.

50. Benchmark for Evaluation of Reactor Simulations, rev. 2.0.1, Massachusetts Institute of Technology (2017).

51. PWR Primary Water Chemistry Guidelines, Volume 1, Revision 4, TR-105714-V1R4, Electric Power Research Institute (1999).

52. W. J. Anderson, BWR Depletion Parameter Sensitivity Evaluation, 32 – 5030781 – 00, Framatome ANP (2003).

53. W. B.J Marshall et al., Axial Moderator Density Distributions, Control Blade Usage, and Axial Burnup Distributions for Extended BWR Burnup Credit, NUREG/CR-7224 (ORNL/TM-2015/544) , US Nuclear Regulatory Commission (2016).

54. Generic Letter 90-02, Supplement 1, "Alternative Requirements for Fuel Assemblies in Design Features Section of Technical Specifications," US Nuclear Regulatory Commission (1992).

55. Safety Analysis Report for the UMS® Universal Transport Cask Docket No. 71-9270 Revision 2, NAC, International (2005).

56. R.E. Ginna Nuclear Power Plant, 2019 10 CFR 50.46 Annual Report, NRC ADAMS ML19098A689 (2019).

57. North Anna Power Station Units 1 and 2 Summary of Facility Changes, Tests and Experiments, NRC ADAMS ML082330474 (2008).

58. K. J. Geelhood, Fuel Performance Considerations and Data Needs for Burnup above 62 GWd/MTU, PNNL-29368, Pacific Northwest National Laboratory (2019).

59. R. Adamson et al., High Burnup Fuel Issues, ZIRET-8 Special Topics Report, Advanced Nuclear Technology International (2003).

60. NAC-UMS® Universal Multi-Purpose Cask System Safety Analysis Report, Revision 2, NAC International (2005).

61. Safety Analysis Report of the HI-STAR 100 Cask System, Revision 15, Holtec International (2014).

62. Review and Prioritization of Technical Issues Related to Burnup Credit for BWR Fuel, NUREG/CR-7158, US Nuclear Regulatory Commission (2012).

63. G. Alonso, S. Bilbao, and E. del Valle, "Impact of the moderation ratio over the performance of different BWR fuel assemblies," *Annals of Nuclear Energy* 85 (2015) 670-678.

64. M. A. Malik et al., Optimization of the Axial Power Shape in Pressurized Water Reactors, DOE/ET/340022-2, Massachusetts Institute of Technology (1981).

65. R. J. Migliore et al., Non-Fuel Assembly Components: 10 CFR 61.55 Classification for Waste Disposal, PNL-10103, US Department of Energy (1994).

66. Control assembly materials for water reactors: Experience, performance and perspectives, Proceedings of a technical committee meeting held in Vienna, 12-15 Oct. 1998, IAEA-TECDOC-1132 (2000).

67. *Safety Evaluation of the General Electric Hybrid I Control Rod Assembly for the BWR4/5 C Lattice,* NRC ADAMS ML20141E616.

68. *Core Design and Operating Data for Cycles 1 and 2 of Peach Bottom 2*, EPRI NP-563, Electric Power Research Institute (1978).

69. J. R. Secker et al., Optimum Discharge Burnup and Cycle Length for PWRs, *Nucl. Technol*. 151:2, 109-119 (2005).

70. R. I. Smith, G. J. Konzek, and W. E. Kennedy, Jr., Technology, Safety and Costs of Decommissioning a Reference Pressurized Water Reactor Power Station, NUREG/CR-0130 Vol1, Battelle Pacific Northwest laboratory, prepared for US Nuclear Regulatory Commission (1978).

71. H. D. Oak et al., Technology, Safety and Costs of Decommissioning a Reference Boiling Water Reactor Power Station, NUREG/CR-0672 Vol2, Battelle Pacific Northwest laboratory, prepared for US Nuclear Regulatory Commission (1979).

72. J. C. Evans et al., Long-Lived Activation Products in Reactor Materials, NUREG/CR-3474, US Nuclear Regulatory Commission (1984).

73. S. B. Ludwig and J. P. Renier, Standard- and Extended-Burnup PWR and BWR Reactor Models for the ORIGEN2 Computer Code, ORNL/TM-11018, Oak Ridge National Laboratory (1990).

74. A. Strasser, High Strength Nickel Alloys for Fuel Assemblies, ZIRAT17 Special Topic Report, A.N.T. International (2012).

75. A. Stasser and P. Ford, IZNA12 Special Topic Report, High Strength Nickel Alloys for Fuel Assemblies, Advanced Nuclear Technology International (2012).

76. X-5 Monte Carlo Team, "MCNP - Version 5, Vol. I: Overview and Theory", LA-UR-03-1987 (2003).

77. A. T. Godfrey, VERA Core Physics Benchmark Progression Problem Specifications, Revision 4, CASL-U-2012-0131-004, Rev 4, Oak Ridge National Laboratory (2014).